

RESTRICTED

FINAL YEAR PROJECT REPORT

Modelling Simulation and Control Design of a 3-DOF Motion Simulator

By

A/C ASHAL AKHTAR

PAK/19094030, 94 (B) EC



ADVISOR

A/P TAIMOOR

CO-ADVISOR

S/L JEHANZAIB

COLLEGE OF AERONAUTICAL ENGINEERING

PAF ACADEMY ASGHAR KHAN, RISALPUR

(AUGUST 2021)

RESTRICTED

RESTRICTED

Modelling Simulation and Control Design of a 3-DOF Motion Simulator

By

PILOT OFFICER ABC

PAK/19094030, 94 (B) EC



ADVISOR

A/P TAIMOOR

CO-ADVISOR

S/L JEHANZAIB

Report submitted in partial fulfillment of the requirements for the degree of Bachelors
of Engineering in Aerospace (BE Aerospace)

In

COLLEGE OF AERONAUTICAL ENGINEERING

PAF ACADEMY ASGHAR KHAN, RISALPUR

(AUGUST 2021)

Approval

It is certified that the contents and form of the project entitled "**Modelling Simulation and Control Design of a 3-DOF Motion Simulator**" submitted by **A/C ASHAL AKHTAR** have been found satisfactory for the requirement of the degree.

Advisor: A/P Taimoor

Signature: _____
Date: _____

Co-advisor : Sqn Ldr Jehanzaib

Signature: _____
Date: _____

RESTRICTED

Dedication

I dedicate this work to my ever-supportive parents who have always believed in me, nourished my spirit, and inspired my efforts; to all my esteemed teachers who guided me through the path of knowledge and wisdom; and to my incredible coursemates, whose camaraderie and assistance were invaluable in crafting this report.

Thank you for standing by me, for the motivation and the countless ways you helped shape this journey and my life. This accomplishment is as much yours as it is mine.

RESTRICTED

Acknowledgement

Embarking on this project was a journey that necessitated guidance and support from various individuals whose insights and assistance have been a bedrock of its success.

First and foremost, I would like to express my deepest gratitude to Assistant Professor Taimoor, who served as my advisor in the final semester and guided me through the critical phases of the project. His supervision and sage advice have been instrumental in shaping the trajectory of this endeavor to its fruitful completion. I am also thankful to Engr. Jehanzaib, my co-advisor, whose expert advice and constructive feedback helped in refining the project to a great extent. A note of thanks is due to Engr. Raja Sohail as well, who provided significant assistance regarding the implementation aspect of my project, offering a reservoir of knowledge and technical know-how.

I extend my heartfelt appreciation to my previous advisor, Dr. Zeashan, whose guidance has been crucial in steering this project to its completion. I am also immensely grateful to the previous Dean of CAE, Tauqeer ul Islam, who articulated the vision that has been the guiding light at every stage of this project.

I am thankful to the creators of SimpleFOC Library and the online forum of SimpleFOC, a community of like-minded individuals sharing knowledge and insights on the Field-Oriented Control Algorithm and their SimpleFOC Library . The support extended by this community has indeed been a pillar of strength, providing a platform where knowledge meets aspiration.

Last but not least, I must express my gratitude to my course mate, Mudassir Riaz, who was a pillar of support during the final assembling of the project, offering fresh perspectives and a helping hand whenever needed.

To all these individuals, and to the many others who have supported me along the way, I extend my deepest thanks. It is through your guidance, support, and belief in this project that it has come to fruition.

Abstract

In the evolving landscape of UAV subsystems development and testing, the implementation of hardware-in-the-loop (HIL) simulation has surged, becoming a cornerstone in the assessment and fine-tuning of flight control computers prone to multi-axial motions. The pivotal element in HIL testing is the 3-degree-of-freedom (3-DOF) rate tables, instrumental in replicating dynamic flight conditions experienced by aircraft.

This report elucidates the comprehensive journey of conceptualizing, designing, and actualizing a 3-DOF rate table, highlighting the critical role played by Euler angle configurations in steering the motor controls precisely aligned with the field-oriented control methodology. The discourse extends to encapsulate the meticulous simulation processes that guided the eventual hardware realization, bringing the envisioned 3-DOF rate table from paper to reality, a critical asset in present and future UAV system developments.

Further, the report ventures to provide a critical analysis of different motor control algorithms and the role of sensors, offering a reflective overview of the project while paving the path for prospective avenues in 3-DOF rate table advancements, a venture at the cusp of modernization with vast potential for future exploration and enhancement.

Table of Contents

1	INTRODUCTION	1
1.1	Project Title	1
1.2	Project Description	1
1.3	Motivation	1
1.4	Scope of the Project	1
1.5	Report Overview	2
2	LITERATURE REVIEW	4
2.1	Motion Simulator	4
2.2	Rate Table	5
2.3	Mechanical Design	6
2.3.1	Parallel Manipulator Mechanism	6
2.3.2	Serial Manipulator Mechanism	7
2.3.3	3-axis Rotary Table	8
2.4	Torque Requirements of the 3-Axis Rate Table	9
2.4.1	Roll Axis	9
2.4.2	Pitch Axis	9
2.4.3	Yaw Axis	9
2.5	Motors	10
2.6	Motor Commutation	12
2.6.1	DC Motors	12
2.6.2	BLDC Motors	12
2.7	Control Strategies for BLDC Motors	12
2.7.1	Pulse Width Modulation (PWM) Control	13
2.7.2	Current Control	13
2.7.3	Voltage Control	13

RESTRICTED

2.7.4	Speed Control	13
2.7.5	Position Control	13
2.7.6	Sensorless Control	13
2.8	Motor Commutation	14
2.8.1	Trapezoidal Commutation	14
2.8.2	Sinusoidal Commutation	18
2.9	Motor Control	18
2.9.1	Field Oriented Control	19
2.9.2	Model Predictive Control (MPC)	22
2.9.3	Direct Torque Control (DTC)	22
2.9.4	Adaptive Control	23
2.9.5	Sliding Mode Control (SMC)	23
2.9.6	Neural Network Control	23
2.9.7	Fractional Order Control (FOC)	23
2.10	Sensors	24
2.10.1	MEMS-based IMUs	24
2.10.2	Dynamometers	24
2.10.3	Optical Encoders	24
2.10.4	Magnetic Encoders	24
2.10.5	Potentiometers	25
2.10.6	Hall Effect Sensors	25
3	Project Approach	26
3.1	Modelling and Simulation	26
3.2	Interfacing with FlightGear (Simulated Rate Table)	26
3.3	Hardware Selection and Procurement	26
3.4	Motor Control	26
3.5	Motor Parameters Tuning	27
3.6	Mechanical Design	27
3.7	Assembling and Interconnecting	27
3.8	Testing and Tweaking	27
3.9	Incorporating IMU	27
3.10	Interfacing with FlightGear (Hardware)	27

4 Euler Angle Configuration	28
4.1 Quaternions	28
4.2 Euler Angles	29
4.3 Body Rate	29
4.4 Euler Angles	29
4.5 Choosing Euler Angles	29
4.6 Conversion from Body Rates to Euler Angles	31
4.7 Simulating Euler Angle Movement	31
4.7.1 Simulation Setup	32
4.7.2 Side-by-Side Visualization	32
4.7.3 Simulation Verification	33
5 Setting Target Specifications for the Rate Table	34
5.1 Angular Freedom	34
5.2 Positional Accuracy	34
5.3 Angular Rates	35
5.4 Load Capacity	35
5.5 Testbed Dimensions	35
5.6 Justification of Specifications	35
6 Hardware Procurement Based on Target Specifications	36
6.1 Gimbal BLDC Motors	36
6.2 Other Procured Hardware	38
6.2.1 Motor Drivers	40
6.3 3D Printing of Frames	42
7 Implementation of Field-Oriented Control (FOC)	44
7.1 Closed-Loop Position Control	44
7.1.1 Torque Loop	44
7.1.2 Velocity Loop	45
7.1.3 Position Loop	45
7.2 Motor Tuning	45
7.2.1 Open Loop Voltage Control	46
7.2.2 Open Loop Velocity Control	46

RESTRICTED

7.2.3	Open Loop Position Control	46
7.2.4	Sensor Integration	46
7.2.5	Closed Loop Controls	46
7.3	Final PID Values	47
7.3.1	Roll Motor	47
7.3.2	Pitch Motor	48
7.3.3	Yaw Motor	48
7.4	Motor Tuning Results	48
7.4.1	Discussion	49
8	Preparing for HILS	54
8.1	IMU MPU-6050 Setup on Testbed	54
8.2	Accessing IMU Values Via WiFi	55
8.3	Hardware in Loop Simulation Block Diagram	55
9	Final Results	56
10	Future Recommendations	58
10.1	Design Adaptations for Heavier Payloads	58
10.2	Lab Equipment for Testing and Validation	58
10.3	Division of Project into Mechanical and Control Design	58
10.4	Integration of Superior Sensors	59
10.5	Utilization of Motors with More Poles	59
10.6	Odrive Motor Controllers	60
10.7	Incorporation of Industrial Slip Rings/Ball Bearings	60
10.8	Integration of High Precision IMU	61
11	Conclusion	62

List of Figures

1.1 A piloted Full Flight Simulator	2
2.1 All six degrees of freedom (6-DOF).	5
2.2 Rate Table	5
2.3 A Sanwood 3-DOF Simulation Table	7
2.4 Ideal Aerospace 1573P Three Axis Positioning and Rate Table System .	7
2.5 A SolidWorks assembly of our rate table	8
2.6 3-axis rate table axes system	8
2.7 DC Servo Motor	10
2.8 Stepper Motor	11
2.9 BLDC Motor	11
2.10 Classification of BLDC Motors	14
2.11 Working of a BLDC Motor	15
2.12 6 MOSFET Switches used for commutation	15
2.13 Trapezoidal functions of the three phases	16
2.14 The commutation zones in trapezoidal control	17
2.15 Switches states corresponding to commutation zones	17
2.16 Speed Tracking in six-step commutation	17
2.17 Sinusoidal vs Trapezoidal single phase current	18
2.18 Stator(magenta) and rotor(grey) magnetic fields	19
2.19 I_q (yellow) and I_d (cyan)	19
2.20 Field Oriented Control using PID controllers	21
2.21 Input Voltage given to 3-phase inverter	21
2.22 An illustration of Model Predictive Control	22
2.23 A depiction of Direct Torque Control	22
2.24 An overview of Sliding Mode Control	23

RESTRICTED

4.1	Visual representation of Quaternions	28
4.2	Intuitive representation of Euler Angles	30
4.3	Euler Angles and Body Rates	31
4.4	Simulation Setup showcasing the integration of SolidWorks model with MATLAB SimScape and FlightGear	32
4.5	Side by Side visualization of Flight Gear and Rate Table Model	33
6.1	Roll and Pitch Motors - Flycat 2805 140kv	38
6.2	Yaw Motor - iPower GM3506	39
6.3	Other Included Hardware	39
6.4	Motor Driver for Roll and Pitch Motor	40
6.5	Motor Driver for Yaw Motor	41
6.6	Components of the 3D Printed Frames	43
6.7	Final Assembly	43
7.1	Torque Loop	44
7.2	Velocity Loop	45
7.3	Position Loop	45
7.4	Yaw Motor (No Load)	49
7.5	Yaw Motor (With Load via Belt-Pulley Configuration)	49
8.1	Location of the IMU MPU-6050 on the testbed	54
8.2	Hardware in Loop Simulation Block Diagram	55
9.1	Integration of Rate Table (Hardware) with Flight Gear	56
9.2	Rate Table Demonstration	57
10.1	Rotary ABZ Encoder	59
10.2	GM-8112 Gimbal Motor with 42 Poles	60
10.3	Odrive Motor Controller	60

Chapter 1

INTRODUCTION

1.1 Project Title

Modelling, Simulation, and Control Design of a 3-DOF Motion Simulator

1.2 Project Description

The aim of this project is to design a 3-axis motion simulator optimized for Hardware-in-the-Loop Simulation (HILS) of Flight Control Computers (FCCs) primarily utilized in UAV subsystems. This simulator will be equipped with an onboard IMU sensor, ensuring a risk-free, economical solution for pre-flight control design evaluation by replicating continuous roll, pitch, and yaw motions, while minimizing communication delays and mechanical lags to achieve precise input tracking.

1.3 Motivation

As UAV systems continue to evolve, the necessity for accurate and reliable testing environments has become paramount. A well-structured 3-DOF motion simulator would facilitate the development process of flight control computers, promising safety and efficiency. The simulator stands as a potential game-changer in the industry, fostering innovation while mitigating risks and reducing costs associated with real-time testing.

1.4 Scope of the Project

Modern day Motion Simulators are complex devices. They are able to generate movement in all of the six degrees of freedom (DOF) that can be experienced by an object.

Manned or Piloted versions have a major role in training, recreation and other augmented reality applications and might find their way in various fields in near future. However they are more mechanically intensive devices. Unmanned platforms also



Figure 1.1: A piloted Full Flight Simulator

have various uses especially in Industries where they are used primarily for sensor tracking and calibration. Rate tables are such equipments. Rate Tables generate roll, pitch and yaw motion of a platform with reference input signals, in a laboratory. This helps cut down the time and cost for product selection and research expenditures. They are also used for calibration and testing of inertial systems, packages or clusters that are sensitive to multiaxial motion. A classic use case is for the Hardware-In-The-Loop simulations(HILS) during development of missiles which help reduce time and cost, by minimizing the number of field trials required. These simulators can also be used for HILS of Inertial Navigation Systems (INS), Attitude Heading Reference Systems (AHRS), flight control systems, Satellite Control Systems, Inertial Measurement Units (IMU) and platform stabilization devices. [1]

1.5 Report Overview

The ensuing chapters are structured as follows to provide a detailed discourse on the project:

Chapter 1: Introduction — This chapter serves as the prologue, offering a glimpse into the project's background, objectives, and scope.

Chapter 2: Literature Review — A critical evaluation of pertinent literature to underpin the theoretical foundations of the project.

Chapter 3: Project Approach — This chapter delineates the strategic approach adopted to navigate through the various phases of the project.

Chapter 4: Euler Angle Configuration — A deep dive into the Euler angle configuration utilized in the simulation process, highlighting its significance and application.

Chapter 5: Setting Target Specifications for Hardware — Detailing the benchmarks and standards established for the hardware components, ensuring efficiency and precision in the simulator's performance.

Chapter 6: Hardware Procurement — This chapter discusses the process undertaken to procure the necessary hardware components, including the selection criteria, vendors, and logistical considerations.

Chapter 7: Field Oriented Control (FOC) — An examination of the principles and applications of FOC in motor control, vital in attaining the desired outcomes in the simulator's functionality.

Chapter 8: Preparing for HILS — Integrating an IMU sensor on the testbed which is integral to the Hardware-in-Loop Simulation (HILS).

Chapter 9: Final Results — Presenting the outcomes achieved, providing a tangible measure of the project's success and insights into potential future developments.

Chapter 10: Future Recommendations — In this chapter, potential pathways for the future development of the project will be outlined. Recommendations for enhancing the current setup, including design modifications for heavier payloads and the integration of more advanced technologies in sensors and motor controllers, will be discussed in detail.

Chapter 11: Conclusion — The concluding chapter summarises the entire project, revisiting the essential points discussed in the earlier chapters and providing a cohesive closure to the report, highlighting the project's relevance to the national needs of Pakistan and how it stands to benefit various industries.

Chapter 2

LITERATURE REVIEW

The conceptualization and construction of motion simulators necessitate a multifaceted approach that hinges significantly on the precision of its mechanical design. This sphere not only dictates the efficacy and reliability of the simulator but also stands as a bulwark ensuring the safety of potential human operators. The literature extant sheds light on diverse avenues of mechanical design, each characterized by a unique set of attributes tailored to meet specific requirements and functionalities. This chapter delves into the intricacies of mechanical designs employed in motion simulators, examining the pivotal role they play in fostering safety and operational efficiency, and the various configurations and mechanisms that stand central to this endeavor.

2.1 Motion Simulator

A motion simulator or motion platform is a mechanism that creates the feelings of being in a real motion environment. Motion platforms are able to generate motion from one to all six degrees of freedom (DOF) that can be experienced by an object that is free to move, such as an aircraft or spacecraft [2]. The six degrees of freedom are three rotational dofs (roll/raw, pitch, yaw) and three linear dofs (surge, heave, sway). Motion platforms may employ parallel manipulator or serial manipulator mechanism

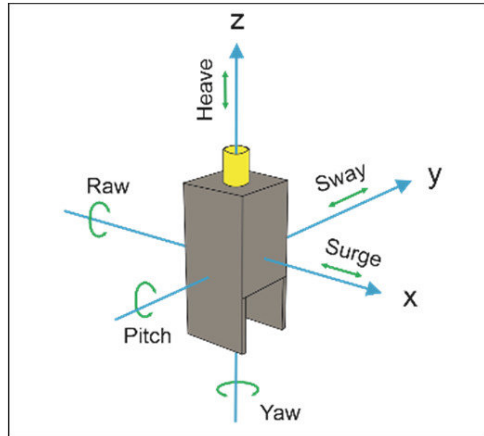


Figure 2.1: All six degrees of freedom (6-DOF).

2.2 Rate Table

A rate table, also known as a motion platform, is primarily engaged in the process of generating rotational motions that meticulously follow the patterns dictated by the input signals received. This makes them a crucial instrument in sensor calibration and testing environments.



Figure 2.2: Rate Table

These tables mainly function through a serial manipulator mechanism, incorporating motors as actuators that work in accordance with the defined input rates. The input rates, essentially being discrete derivatives of Euler angles, are determined through a

systematic analysis of various aspects including the roll angle, attitude, and heading of the test system.

An important differentiation in rate tables comes from the kind of motors utilized for actuation. Slow, heavy-duty rate tables generally employ stepper motors, whereas their faster counterparts make use of feedback servos. This choice of motors significantly impacts the rate table's performance in terms of speed and precision.

Moreover, rate tables can be equipped with slip rings, a feature that enables continuous 360-degree rotation about all three axes, broadening the spectrum of tests that can be performed using a rate table.

However, despite the array of functionalities that rate tables offer, they come with their own set of challenges. One prominent issue is the trade-off between angular velocity, positional accuracy, and the payload capacity. These parameters are inherently interlinked, and optimizing one aspect can often lead to compromises in the others. Furthermore, being serial manipulators, rate tables are subject to Gimbal Lock, a phenomenon that restricts the motion at certain orientations, adding a layer of complexity in their operation.

In conclusion, rate tables stand as a pivotal tool in the realm of sensor testing and calibration, offering a rich set of functionalities while bringing along certain challenges that warrant meticulous attention in the design and operation phases to fully leverage their capabilities.

2.3 Mechanical Design

Mechanical design is a critical component in developing motion simulators, especially concerning safety and functionality. While these simulators sometimes involve human users, in the context of rate tables, the focus shifts to achieving optimal reliability and accuracy in testing. There are predominantly two configurations; parallel and serial manipulator mechanisms.

2.3.1 Parallel Manipulator Mechanism

This mechanism employs a series of computer-controlled chains to support a single platform, fostering flexibility and accuracy in gadgets such as flight simulators. Its

hallmark is the ability to facilitate 6-DOF motion, albeit within the actuators' physical constraints, which limits its rotational scope, hindering continuous 360-degree movement [3, 4].



Figure 2.3: A Sanwood 3-DOF Simulation Table

2.3.2 Serial Manipulator Mechanism

Prominently featured in industrial robots, this mechanism relies on a series of joints and actuators forming a kinematic chain to support rotational movements. It facilitates continuous rotational movement around three axes, contingent upon the integration of slip rings to circumvent wire entanglement and centralizing the system's gravity center to reduce torque demands [4].



Figure 2.4: Ideal Aerospace 1573P Three Axis Positioning and Rate Table System

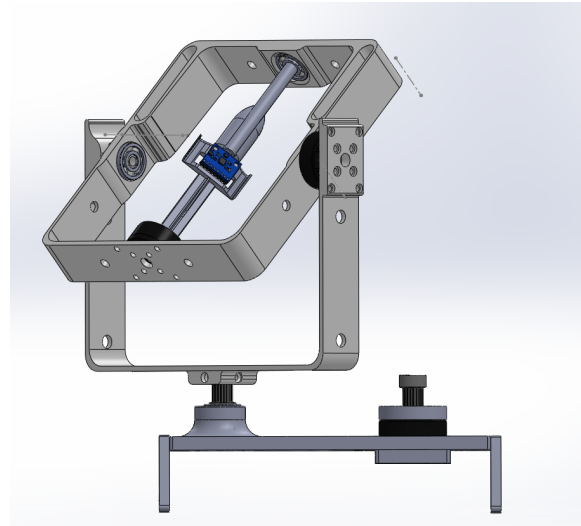


Figure 2.5: A SolidWorks assembly of our rate table

2.3.3 3-axis Rotary Table

This table involves three torque motors steering the roll, pitch, and yaw rotational axes, each denoted as **r**, **p**, and **n**. The relationship between the platform and gimbal frame is depicted through a rotation matrix dependent on motor angles symbolized as ϕ , θ , and ψ .

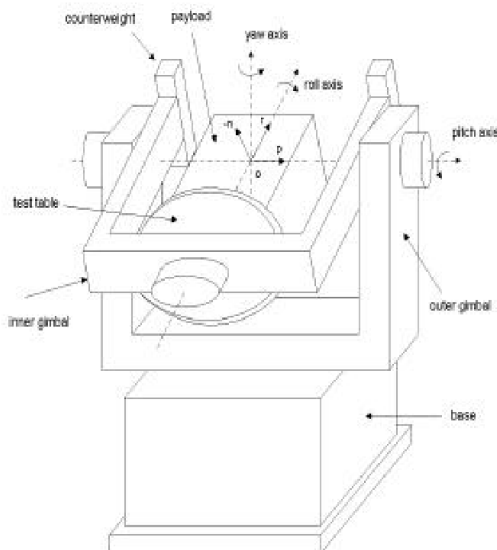


Figure 2.6: 3-axis rate table axes system

$$R_n^r = \begin{bmatrix} c_\phi c_\theta & -s_\phi c_\psi + c_\phi s_\theta s_\psi & s_\phi s_\psi + c_\phi s_\theta c_\psi \\ s_\phi c_\theta & c_\phi c_\psi + s_\phi s_\theta s_\psi & -c_\phi s_\psi + s_\phi s_\theta c_\psi \\ -s_\theta & c_\theta s_\psi & c_\theta c_\psi \end{bmatrix} \quad (2.1)$$

where the variables represent the respective cosines and sines of the angles [5].

An intricate balance between the payload specifications and material selection for frames and motors remains pivotal in the design phase, necessitating meticulous planning before venturing into fabrication to preclude potential hurdles in physical setup alterations.

2.4 Torque Requirements of the 3-Axis Rate Table

In order to accurately simulate different motion profiles, it is important to calculate the torque requirements of each motor.

2.4.1 Roll Axis

The roll axis consists of a test table, payload, and roll motor. The moment of inertia of the roll part is denoted by J_r , and the roll angle is denoted by ϕ . The torque requirement for the roll motor can be calculated as:

$$T_r = J_r \ddot{\phi} \quad (2.2)$$

where $\ddot{\phi}$ is the roll acceleration.

2.4.2 Pitch Axis

The pitch axis consists of an inner gimbal, counterweights, and pitch motor. The moment of inertia of the pitch part is denoted by J_p , and the pitch angle is denoted by θ . The torque requirement for the pitch motor can be calculated as:

$$T_p = J_p \ddot{\theta} - J_r \ddot{\phi} \sin \theta \quad (2.3)$$

where $\ddot{\theta}$ is the pitch acceleration.

2.4.3 Yaw Axis

The yaw axis consists of an outer gimbal and yaw motor. The moment of inertia of the yaw part is denoted by J_y , and the yaw angle is denoted by ψ . The torque requirement for the yaw motor can be calculated as:

$$T_y = J_y \ddot{\psi} - J_r \ddot{\phi} \cos \theta \quad (2.4)$$

where $\ddot{\psi}$ is the yaw acceleration. [5]

2.5 Motors

Rate tables typically use one or more actuators to provide the necessary motion to simulate the aircraft's behavior. The most common types of actuators used in rate tables with respect to motion are:

- Linear Actuators
- Rotary Actuators

and with respect to motion generation:

- Pneumatic Actuators
- Hydraulic Actuators
- Electric Actuators

Electric Rotary actuators or motors are our choice due to their ease of availability and controllability. There are three main motor types used for control applications:

- Servo Motors
- Stepper Motors
- BLDC Motors



Figure 2.7: DC Servo Motor

Traditional DC motors are cheaper and controlling them is easier. However, they do not provide good positional tracking. Servo Motors, which are DC Motors with

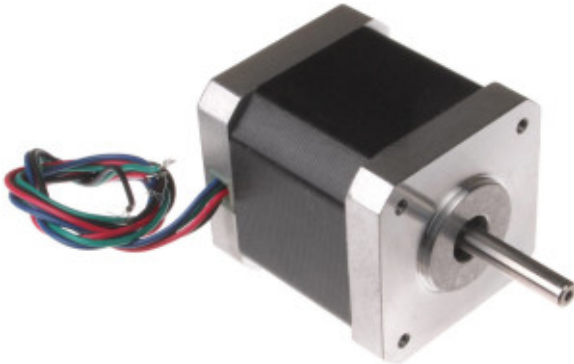


Figure 2.8: Stepper Motor



Figure 2.9: BLDC Motor

feedback servo mechanisms, have good positional tracking but poor rate tracking, and most of them generate less torque. Stepper Motors have good positional and rate tracking and also generate very large torques. However, they do not provide smooth high speeds, which are required for our rate table operation. [6]

Brushless DC Motors

A BLDC motor consists of a permanent magnet-based rotor and polyphase armature windings-based stator in an in-runner BLDC (vice-versa in out-runner). It varies from a typical DC motor in that it lacks brushes and commutation is carried out electronically with the aid of an electronic drive that supplies the stator windings. BLDC motors have good speed tracking. Position control can be implemented using encoders or observer feedback loops. However, they have complex control. The torque to speed ratio depends on the number of windings on the stator. [7] Some other features of brushless motors are:

- High Precision

- High Efficiency
- Low Maintenance
- High Reliability
- High Speeds
- Long Life

2.6 Motor Commutation

The motor control circuits of traditional DC Motors are simple and easy to implement. However, due to brushes, they are not as reliable. Brushless DC Motors, as the name suggests, are without brushes and achieve commutation electronically through electronic drives. This makes them more reliable but also increases complexity in their control.

2.6.1 DC Motors

In a DC motor, commutation is achieved by means of a commutator and brushes. This means that the direction of the current and hence the magnetic field is always in a direction to produce rotation. The speed of a DC motor is proportional to the voltage applied across its terminals and can be controlled by varying the voltage supply.

2.6.2 BLDC Motors

In a BLDC motor, commutation is achieved electronically. This is done with the help of a drive that supplies the three stator windings with current in a sequence determined by the rotor position. The rotor position can be sensed using Hall effect sensors or determined using a sensorless control algorithm.

2.7 Control Strategies for BLDC Motors

- Pulse Width Modulation (PWM) Control
- Current Control

- Voltage Control
- Speed Control
- Position Control
- Sensorless Control

2.7.1 Pulse Width Modulation (PWM) Control

PWM control is the most widely used control method for BLDC motors. It involves modulating the duty cycle of the pulses to control the average voltage applied to the motor.

2.7.2 Current Control

Current control involves controlling the current flowing through the motor windings to control the torque produced by the motor.

2.7.3 Voltage Control

Voltage control involves controlling the voltage applied across the motor terminals to control its speed.

2.7.4 Speed Control

Speed control involves controlling the speed of the motor through feedback loops to maintain a desired speed set point.

2.7.5 Position Control

Position control involves controlling the position of the motor shaft to a desired position through feedback loops.

2.7.6 Sensorless Control

Sensorless control involves controlling the motor without any feedback sensors. This is achieved through observer feedback loops or back-EMF sensing.

2.8 Motor Commutation

The motor control circuits of traditional DC Motors are simple and easy to implement. However due to brushes they are not as reliable. Brushless DC Motors are as name suggests without brushes and achieve commutation electronically by applying a three phase voltage at different rotor positions. BLDC Motors having permanent magnet rotor and 3-phase stator are in-runner bldc motors. Whereas those having 3-phase rotors and permanent magnet stators are out-runner. The windings for high speed low torque motors are delta wound whereas windings for low speed high torque motors are wye-wound with a common neutral point. Hence their control systems have added

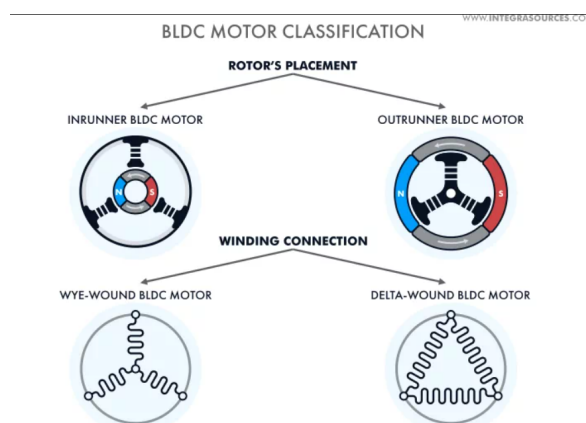


Figure 2.10: Classification of BLDC Motors

complexity of having a 3-phase power supply and knowing the rotor position in order to align the applied voltage. [8]. The rotors position is determined through hall sensors, encoders or back emf from the motor. The windings are energised to form electromagnets which attract the permanent magnet as soon as the rotor position changes the electronic commutation switches the windings and the rotor is attracted to the next winding and so on. Hence the rotor is kept chasing the changing magnetic field of the stator. BLDCs have a trapezoidal back-emf and are commonly controlled by trapezoidal control. However BLDC Motors having a sinusoidal back emf are referred as PMSM or Permanent Magnet Synchronous Motors. [9]

2.8.1 Trapezoidal Commutation

Trapezoidal Commutation is also called Six Step Commutation. In this approach six switches are used to do commutation every 60 degrees. These switches form an

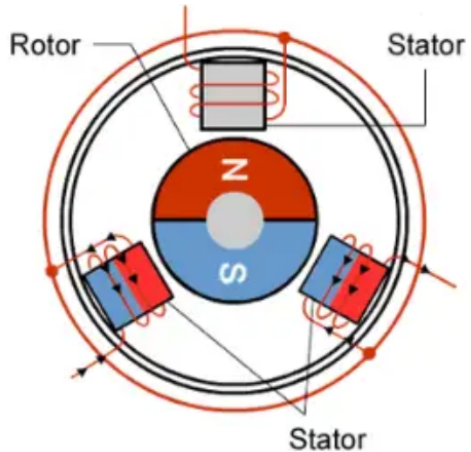


Figure 2.11: Working of a BLDC Motor

inverter which converts our DC to 3-phase supply hence the DC in BLDC. [10] The

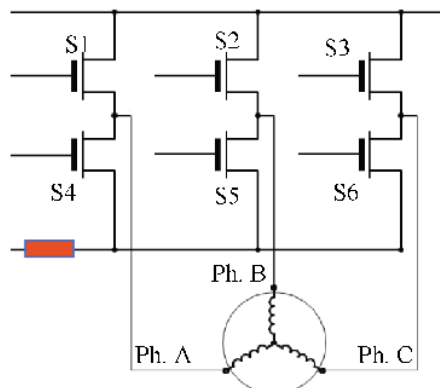


Figure 2.12: 6 MOSFET Switches used for commutation

mathematical equations defining this model are as follows: Assuming winding resistances to be R_a , R_b and $R_c = R$ for a balanced system

$$V_a = Ri_a + (L - M)\frac{di_a}{dt} + e_a \quad (1)$$

$$V_b = Ri_b + (L - M)\frac{di_b}{dt} + e_b \quad (2)$$

$$V_c = Ri_c + (L - M)\frac{di_c}{dt} + e_c \quad (3)$$

Where V_a , V_b , V_c are the terminal phase voltages. i_a , i_b , i_c are the stator phase currents, R the armature resistance, L the self inductance of stator windings and M the mutual inductance between them and e_a , e_b , e_c is the back emf generated. [11] Where the back emfs are related to angular velocity ω as follows

$$e_a = K_w f(\theta_e) \omega \quad (4)$$

$$e_b = K_w f(\theta_e - \frac{2\pi}{3}) \omega \quad (5)$$

$$e_c = K_w f(\theta_e + \frac{2\pi}{3}) \omega \quad (6)$$

Here K_ω is the back emf constant of the motor and f gives the trapezoidal function of phase A. The functions of each phase are 120 degrees apart as shown in the figure below.

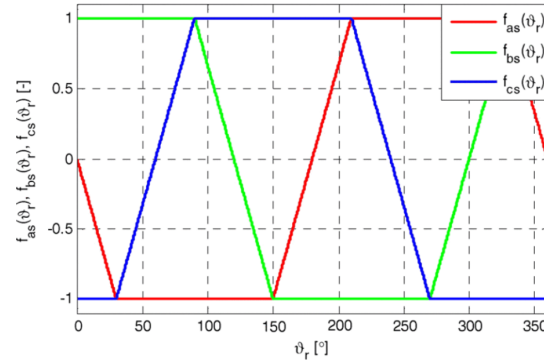


Figure 2.13: Trapezoidal functions of the three phases

The torque generated is as follows [12]

$$\tau_e = pK_\omega [f_{as}(\theta_e)i_a + f_{bs}(\theta_e)i_b + f_{cs}(\theta_e)i_c] \quad (9)$$

The torque generated is due to the Lorentz force acting on rotor due to stator field and is hence proportional to the cross product of rotor and stator magnetic fields. So the rotor magnetic field moves to align itself at 0 degrees w.r.t the stator magnetic field but the torque generated is maximum at 90 degrees.

In 6-step commutation the rotor enters the new commutation zone at 120 degrees is attracted till 60 degrees where it enters a new commutation zone at 120 degrees. Hence the angle between stator and rotor magnetic fields fluctuates between 60 and 120 degrees which gives us the trapezoidal back emf. If we increase the number of pole pairs we decrease the commutation zones. For e.g for 2 pole-pairs we have a

RESTRICTED

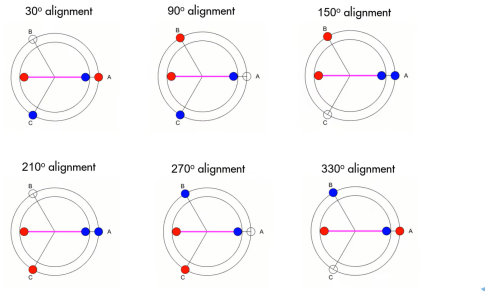


Figure 2.14: The commutation zones in trapezoidal control

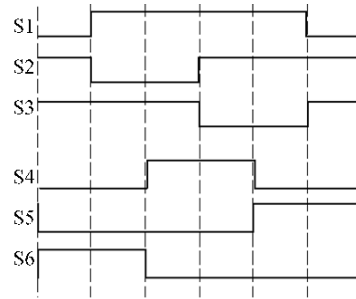


Figure 2.15: Switches states corresponding to commutation zones

30 degree commutation zone and for 4 pole-pairs we have a 15 degree commutation zone. However the relative angle still fluctuates between 82.5 degrees to 97.5 degrees which causes ripples torque generation, noisier rotation and unreliability. In case of speed tracking the motor velocity shifts between two velocities and in case of position tracking it jitters back and forth over the required position. This jerkiness can occasionally cause unwelcome vibrations and mechanical noise which will pose problems in our rate table design. [13]

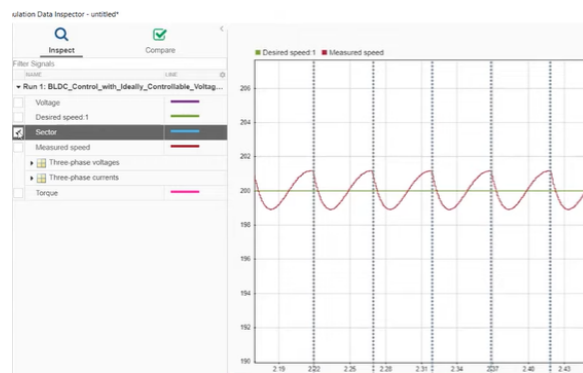


Figure 2.16: Speed Tracking in six-step commutation

2.8.2 Sinusoidal Commutation

The ripples in the torque generated can be removed using sinusoidal Commutation, which is sinusoidally synced by the drive, distributes current in the shape of a sinewave through each of the motor's three phases. There must be 120 electrical degrees between each sinewave. It requires proper overlap of the phase switching, or the selective firing of many pairs of MOSFET switches at once. [14] The resultant flux can then be changed in a more continuous manner, resulting in a smoother motor rotation, by carefully modulating the current flow into each of the three phases. Although there may

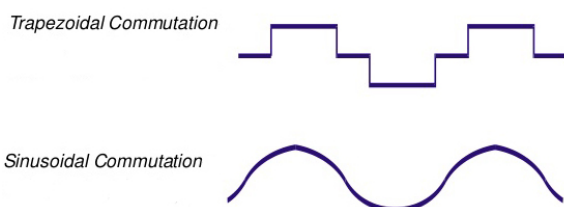


Figure 2.17: Sinusoidal vs Trapezoidal single phase current

be some torque ripple due to algorithmic commutation imperfections, winding uniformity, magnet placement variation, magnet width and strength variation, and non-zero ADC drive offset voltages, in theory there is zero torque ripple because the current is sinusoidal and there are no discontinuities in the current flow. Trapezoidal commutation using hall sensors is frequently utilised at motor startup, switching to Sinusoidal commutation after few duty cycles. This is because the motor control algorithms for this commutation require the stator magnetic field to be exactly 90 degrees from rotor magnetic field for maximum torque generation. Hence a rotary encoder is required to know the position of rotor in this motor commutation configuration.

2.9 Motor Control

High efficiency from BLDC motors can be achieved using electronic commutation techniques as discussed above. Simple trapezoidal control is suitable for low-speed applications whereas sinusoidal control is suitable for high-speed applications and requires more complex hardware and software. For high-performance applications we require control algorithms that are more robust and produce desired results. For controllability applications several motor control techniques are implemented which have different

applications.

2.9.1 Field Oriented Control

Field Oriented Control (FOC) is a technique for controlling the speed and torque of a three-phase AC electric motor, including Brushless DC (BLDC) motors, Permanent Magnet Synchronous Motors (PMSM), and AC Induction Motors (ACIM). FOC works by separating the motor's magnetic field into two components: the flux component(I_d) also called the direct component and the torque component(I_q) alled the quadrature component . By controlling the two components independently, FOC can achieve high levels of efficiency and precision control. For acheiving maximum torque our rotor and stator field must be at 90 degrees to each other. Thus for achieving constant high torque we must minimize our direct component and maximize our quadrature component. However the flux component can be used to regulate the torque and produce the desired performance.

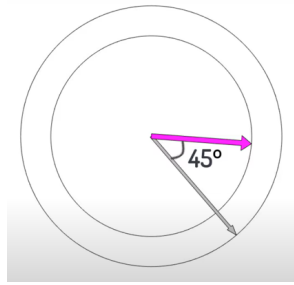


Figure 2.18: Stator(magenta) and rotor(grey) magnetic fields

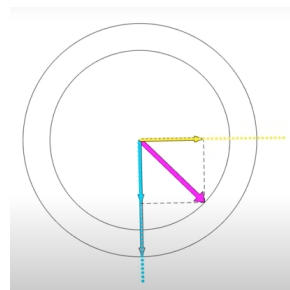


Figure 2.19: I_q (yellow) and I_d (cyan)

Field oriented control is carried out in the following steps

- Measure rotor angular position
- Compute desired stator field vector
- Control 3-phase currents to achieve desired stator field vector

The stator field currents i_a , i_b and i_c are converted to direct and quadrature components using Clarke and Park Transform. The Clarke and Park transforms are mathematical techniques used in electrical engineering to convert three-phase electrical quantities (such as currents and voltages) into two-phase representations. These

transforms are commonly used in the control of three-phase electric machines such as AC induction motors and permanent magnet synchronous motors.

The Clarke transform maps the three-phase currents or voltages to a two-phase representation in a rotating reference frame. The two-phase representation is composed of two orthogonal components, one in phase with the original three-phase quantities and the other 90 degrees out of phase. The Clarke transform is defined as:

$$\begin{bmatrix} i_\alpha \\ i_\beta \end{bmatrix} = \begin{bmatrix} 1 & -\frac{1}{2} & -\frac{1}{2} \\ 0 & \frac{\sqrt{3}}{2} & -\frac{\sqrt{3}}{2} \\ \frac{1}{2} & \frac{1}{2} & \frac{1}{2} \end{bmatrix} \begin{bmatrix} i_a \\ i_b \\ i_c \end{bmatrix}$$

where i_a , i_b , and i_c are the three-phase currents, and i_α and i_β are the two-phase currents.

The Park transform, also known as the dq0 transform, is a transformation of a set of two-phase variables from a stationary frame of reference to a rotating frame of reference. The Park transform is often used in the control of electric machines, as it simplifies the analysis of the machine behavior in the rotating reference frame. The Park transform is defined as:

$$\begin{bmatrix} i_d \\ i_q \end{bmatrix} = \begin{bmatrix} \cos \theta & \sin \theta \\ -\sin \theta & \cos \theta \end{bmatrix} \begin{bmatrix} i_\alpha \\ i_\beta \end{bmatrix}$$

where i_α and i_β are the two-phase currents in the stationary reference frame, i_d and i_q are the two-phase currents in the rotating reference frame, and θ is the electrical angle between the two frames. [9]

These i_d and i_q can then be controlled using control techniques such as PID control to achieve the desired torque/flux. These controllers generate v_q and v_d which can be translated to three phase voltages using Inverse Clarke/Park transforms. The three phase voltages are used to generate three phase currents using the inverters. These currents are used to drive a BLDC Motor using Field Oriented Control.

Field Oriented Control is implemented with two modulation schemes

- SVPWM (Space Vector Pulse Width Modulation)
- SPWM (Sinusoidal Pulse Width Modulation)

Both of these modulation schemes differ in the way they do the switching in the 3-phase inverter. In SPWM the 3 phase voltages given to the inverter are sinusoidal. Whereas

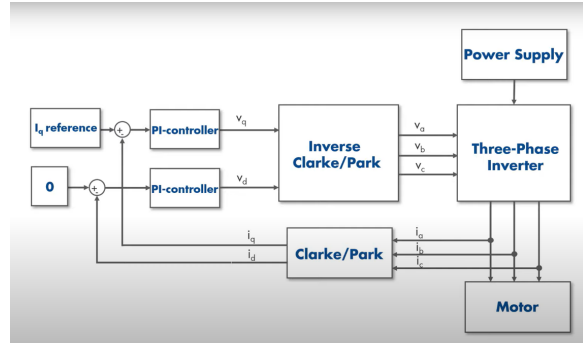


Figure 2.20: Field Oriented Control using PID controllers

in SVM or SVPWM the 3-phase voltages are sinusoidal with a double hump.

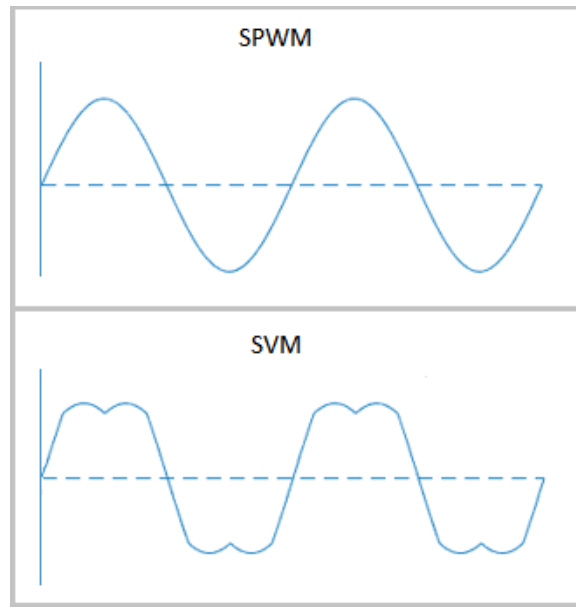


Figure 2.21: Input Voltage given to 3-phase inverter

With a sine wave as the expectation of the output waveform, SPWM works using a sine wave and a triangle wave respectively as the modulation wave and the carrier. The modulation has the same frequency as the desired sine wave while the carrier has a much higher one. Compare the modulation with the carrier, when they intersect, take their intersections as on-off times of the switches, then we can obtain an isometric, continuous, pulse width varying sequence, which are arranged in width according to the sine law. [9] The main objective of SPWM control is to achieve an inverter output voltage that closely approximates a sine wave, disregarding the output current waveform. On the other hand, SVM prioritizes generating a constant-magnitude rotating magnetic field for the motor from the motor's perspective. This method treats the inverter and motor as a single unit, resulting in a straightforward model that is suitable

for real-time control by microprocessors [15].

Although Field Oriented Control is the most efficient and general motor control algorithm there are some advance motor control techniques that are developed over the years.

2.9.2 Model Predictive Control (MPC)

This advanced control technique uses a mathematical model of the motor and a cost function to predict future behavior and optimize control actions. MPC can handle complex systems and constraints, making it useful for high-performance applications.

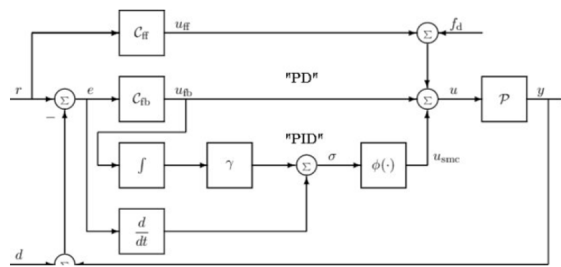


Figure 2.22: An illustration of Model Predictive Control

2.9.3 Direct Torque Control (DTC)

This technique also uses a mathematical model to control the motor's torque directly. The control scheme is based on a hysteresis band, and the system attempts to keep the actual torque within this band.

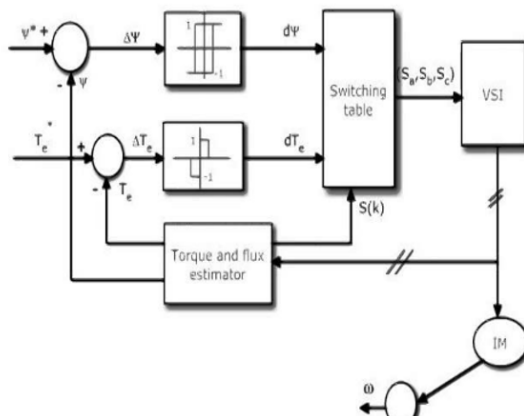


Figure 2.23: A depiction of Direct Torque Control

2.9.4 Adaptive Control

This technique adjusts the control parameters in real-time based on the changing motor dynamics and operating conditions. Adaptive control can improve the motor's performance, efficiency, and robustness under varying loads and disturbances.

2.9.5 Sliding Mode Control (SMC)

This technique applies a sliding surface to the control system to ensure robustness against model uncertainties and external disturbances. SMC can provide fast and accurate control, but it may require tuning to minimize chattering.

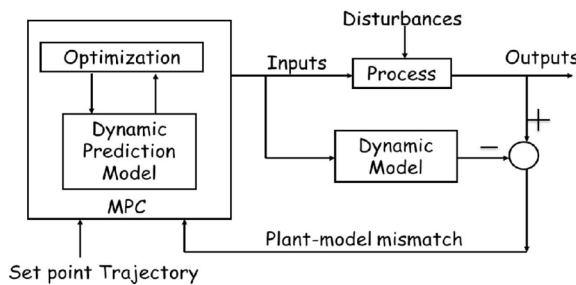


Figure 2.24: An overview of Sliding Mode Control

2.9.6 Neural Network Control

This technique uses an artificial neural network to learn the motor's behavior and generate the control signals. Neural network control can adapt to changing conditions and provide high accuracy control, but it may require more computational resources and training data.

2.9.7 Fractional Order Control (FOC)

This technique applies fractional calculus to the motor control system, enabling more precise control of the motor dynamics. FOC can improve the motor's performance, stability, and efficiency, but it may require more complex mathematical modeling and analysis. [16]

2.10 Sensors

Sensors are devices that detect and respond to physical or chemical stimuli from the environment, converting them into measurable signals that can be processed and analyzed. Sensors are required in rate tables for measuring and detecting various physical quantities, such as angular position, velocity, acceleration, and torque, to provide feedback for controlling and adjusting the motion of the table in real-time.

2.10.1 MEMS-based IMUs

MEMS-based Inertial Measurement Units (IMUs) are sensors that measure and report linear and angular accelerations and rates, often with a combination of microelectromechanical systems (MEMS) gyroscopes and accelerometers. MEMS-based IMUs are commonly used in 3-axis rotary tables for motion control, as they provide precise and accurate measurements of motion.

2.10.2 Dynamometers

A dynamometer is a sensor used to measure the torque and rotational speed of a rotating shaft. It can be used to measure the mechanical power output of an engine, motor, or other rotating machinery. In the context of 3-axis rotary tables, dynamometers can be used to measure the torque required to rotate the table, and the rotational speed of the table.

2.10.3 Optical Encoders

Optical encoders are sensors that use light to detect changes in position, typically through a patterned disk that rotates with the shaft being measured. As the disk rotates, the light passes through the pattern and is detected by a photodetector. This allows the encoder to determine the rotation angle and speed of the motor shaft.

2.10.4 Magnetic Encoders

Magnetic encoders are similar to optical encoders, but instead of using light, they use magnetic fields to detect position. They are typically more robust than optical encoders and can be used in harsh environments.

2.10.5 Potentiometers

A potentiometer is a variable resistor that can be used to measure changes in position or angle. It consists of a resistive element and a sliding contact that moves along the element as the shaft rotates.

2.10.6 Hall Effect Sensors

Hall effect sensors use a magnetic field to detect changes in position or proximity. They are commonly used in proximity sensors, speed sensors, and position sensors. Hall effect sensor are typically used in conventional BLDC drives.

Chapter 3

Project Approach

3.1 Modelling and Simulation

This section covers the modelling and simulation aspect of the project. Details about the approaches and methods used in the modelling and simulation phase will be discussed here.

3.2 Interfacing with FlightGear (Simulated Rate Table)

In this section, we delve into the interfacing of the project with FlightGear focusing on the simulated rate table. The methods, challenges, and results of this interfacing will be explored.

3.3 Hardware Selection and Procurement

This section will focus on the criteria for selecting hardware and the process of procurement. Details about the different hardware components chosen and the reasons behind these choices will be discussed.

3.4 Motor Control

This section is dedicated to motor control, discussing the different control algorithms, strategies, and technologies that have been employed in the project to ensure optimal motor control.

3.5 Motor Parameters Tuning

In this section, the tuning of motor parameters is discussed. Here, we will delve into the techniques used for tuning and the results obtained from different tuning approaches.

3.6 Mechanical Design

This section covers the mechanical design aspect of the project. It will discuss the conceptualization and realization of the mechanical components, focusing on the design principles and considerations that guided the mechanical design process.

3.7 Assembling and Interconnecting

This section describes the process of assembling and interconnecting various components. It encompasses the practical approaches undertaken to ensure seamless assembly and interconnection of different elements in the project.

3.8 Testing and Tweaking

This section will focus on the testing phase of the project, discussing the methodologies employed in testing, and the tweaking processes undertaken to refine the project components for optimal performance.

3.9 Incorporating IMU

Here, we discuss the integration of the Inertial Measurement Unit (IMU) into the project, covering the functionalities it brings and how it has been incorporated to enhance the project's capabilities.

3.10 Interfacing with FlightGear (Hardware)

In this final section, we focus on the interfacing of the project with FlightGear, this time concentrating on the hardware aspect. It will cover the procedures, challenges, and results obtained from this interfacing phase.

Chapter 4

Euler Angle Configuration

Euler angles offer a way to represent the orientation of an object using three angles. In the context of UAVs, they are critical for understanding and controlling the aircraft's orientation.

4.1 Quaternions

Quaternions provide a way to represent rotations in a four-dimensional space. They are more complex than Euler angles but can be used to describe any orientation without suffering from gimbal lock.

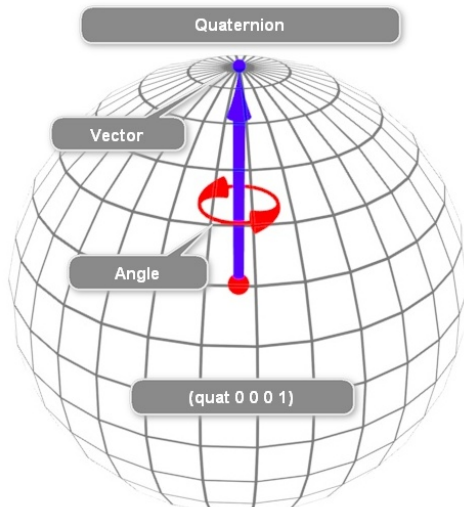


Figure 4.1: Visual representation of Quaternions

4.2 Euler Angles

Euler angles, often denoted as ϕ , θ , and ψ , are three angles that describe an object's orientation in three-dimensional space. They are particularly useful for UAVs that don't undergo gimbal lock, as they can be easily mapped to motor configurations.

4.3 Body Rate

The body rate describes the rate of change of the UAV's orientation. It's crucial for understanding how fast the UAV is changing its position in its own reference frame. They are represented by p, q and r values and change with its own reference frame. They are closely related to flight dynamics.

4.4 Euler Angles

Euler angles, often denoted as ϕ , θ , and ψ , are three angles that describe an object's orientation in three-dimensional space. They are particularly useful for UAVs that don't undergo gimbal lock, as they can be easily mapped to motor configurations.

4.5 Choosing Euler Angles

Euler angles, described by the roll (ϕ), pitch (θ), and yaw (ψ), present a straightforward and intuitive method to express an object's orientation in three-dimensional space. In the context of our UAV design and mission profile, there are several reasons why Euler angles are our preferred choice for orientation representation:

- 1. Simplicity and Intuitiveness:** Euler angles directly map to physical rotations around the UAV's body axes. This makes them intuitively easier to visualize, understand, and debug.
- 2. Motor Configuration:** Our UAV has its motors configured in a manner that aligns with the Euler axes. This means each motor directly influences a specific Euler angle, simplifying control mechanisms and ensuring swift, responsive maneuvers.

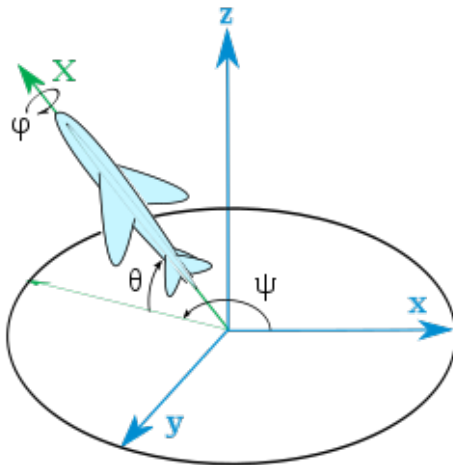


Figure 4.2: Intuitive representation of Euler Angles

3. **Avoidance of Gimbal Lock:** Gimbal lock is a situation where one of the rotation axes aligns with another, causing a loss of a degree of freedom. While this is a limitation of Euler angles in some scenarios, our UAV's operational envelope and design ensure it doesn't undergo extreme orientations leading to gimbal lock. This means we can leverage the benefits of Euler angles without the typical associated risks.
4. **Computational Efficiency:** For systems where rapid processing is essential, like real-time UAV control, the computational simplicity of Euler angles compared to alternative orientation representations (like quaternions) can lead to quicker response times.
5. **Ease of Integration:** Many control algorithms, especially classical ones, are developed and described using Euler angles. Using them directly can simplify the integration of existing control methodologies and reduce the need for transformations.

While there are other methods of representing orientation, such as quaternions or rotation matrices, for the specific design, mission profile, and operational conditions of our UAV, Euler angles provide a harmonious balance of simplicity, intuitiveness, and computational efficiency.

4.6 Conversion from Body Rates to Euler Angles

Understanding how to convert body rates to Euler angles is essential in UAV dynamics as it allows for precise control and stabilization of the UAV during flight. In this section, we elaborate on the mathematical formulations and practical applications of this conversion. The transformation from body rates (p, q, r) to Euler angle rates $(\dot{\phi}, \dot{\theta}, \dot{\psi})$ can be represented by the following matrix equation:

$$\begin{bmatrix} \dot{\phi} \\ \dot{\theta} \\ \dot{\psi} \end{bmatrix} = \begin{bmatrix} 1 & \sin \phi \tan \theta & \cos \phi \tan \theta \\ 0 & \cos \phi & -\sin \phi \\ 0 & \sin \phi \sec \theta & \cos \phi \sec \theta \end{bmatrix} \begin{bmatrix} p \\ q \\ r \end{bmatrix}$$

where (ϕ, θ, ψ) are the Euler angles and (p, q, r) are the body rates.

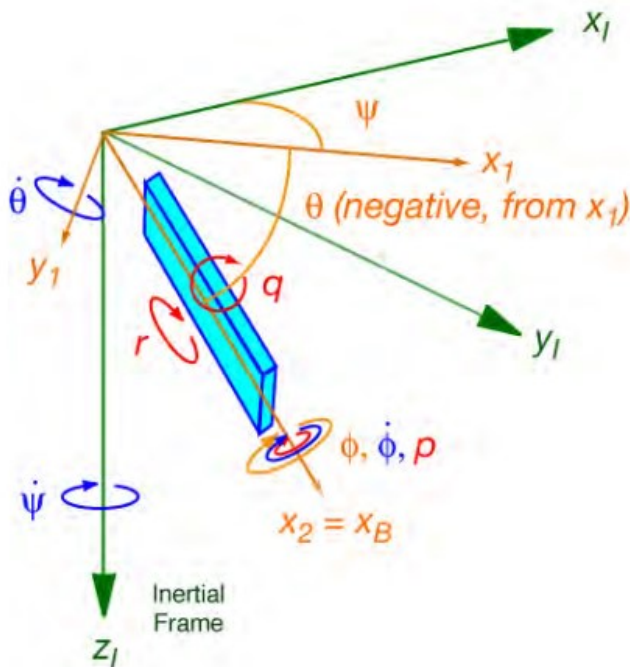


Figure 4.3: Euler Angles and Body Rates

4.7 Simulating Euler Angle Movement

In this section, we delve into the simulation aspect of Euler angle movement, focusing on how identical Euler angles can be relayed to both the rate table simulated model in SimScape and flight gear simulation. Ensuring that the aircraft orientation remains consistent across both platforms is a pivotal part of the process.

4.7.1 Simulation Setup

We have used a simplistic SolidWorks model of our rate table, which was imported into MATLAB SimScape to facilitate the simulation process. The simulation setup was orchestrated meticulously to ensure accurate representation and synchronization of Euler angles derived from our flight dynamics model. These angles are fed simultaneously to both the rate table simulated in SimScape and the FlightGear simulation, serving as a cornerstone in our setup. The configuration ensures that any change in the angles is reflected instantaneously across both platforms, thereby maintaining a high fidelity simulation environment.

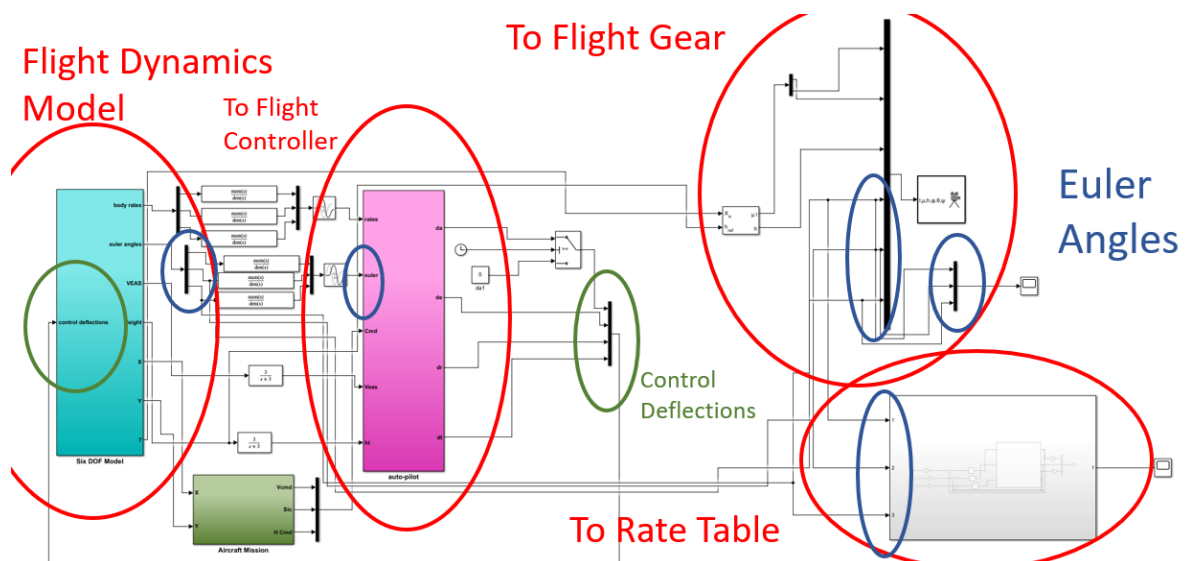


Figure 4.4: Simulation Setup showcasing the integration of SolidWorks model with MATLAB SimScape and FlightGear

4.7.2 Side-by-Side Visualization

A crucial part of verifying the simulation is to have a side-by-side visualization of both the Flight Gear and the rate table model. This comparative visualization facilitates an accurate and efficient validation of the aircraft orientation on both platforms. The side-by-side representation is designed to validate the synchronized movement and alignment of the Euler angles on both the platforms.

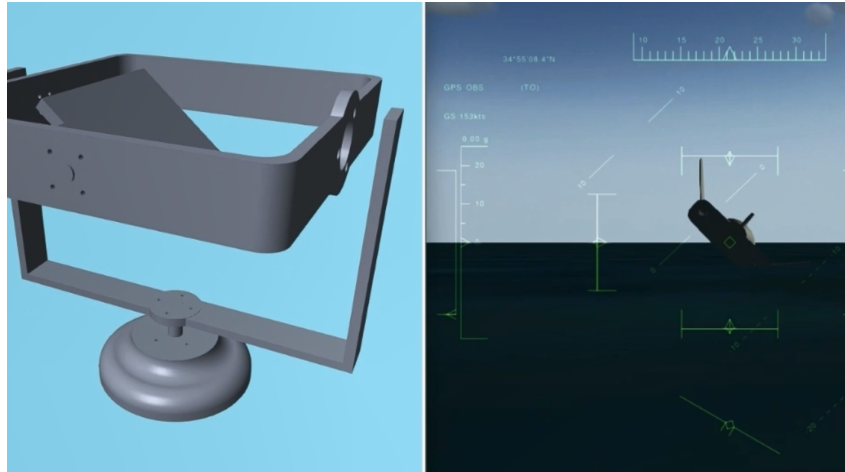


Figure 4.5: Side by Side visualization of Flight Gear and Rate Table Model

4.7.3 Simulation Verification

During the simulation verification stage, the same set of Euler angles are sent to both simulation environments. The steps involved are as follows:

1. **Input Euler Angles:** The Euler angles, ϕ , θ , and ψ , are input into both the Sim-Scape rate table simulated model and the flight gear simulation.
2. **Monitoring Real-Time Changes:** In real-time, changes in the orientation of the UAV are monitored meticulously in both environments to ensure consistency.
3. **Comparative Analysis:** A comparative analysis is conducted post-simulation to confirm the veracity of the Euler angles depicted in both simulations.
4. **Fine-Tuning:** Based on the comparative analysis, necessary fine-tuning is done to eliminate any discrepancies in the future simulations.

By adhering to the above methodology, we ensure that the Euler angle representation in both environments is harmonized, paving the way for reliable and accurate simulations in the future.

Chapter 5

Setting Target Specifications for the Rate Table

In this chapter, we outline the target specifications for the rate table intended to test the Flight Control Computer (FCC) of our UAV. The specifications are designed to emulate the flight dynamics of high-speed target drones, such as kamikaze drones, to ensure the UAV can withstand and operate optimally in conditions mimicking real-world scenarios. Further, we selected the load capacity and testbed dimensions to accommodate a generic Microcontroller Unit (MCU) for flight control, specifically, a Raspberry Pi.

5.1 Angular Freedom

To facilitate a comprehensive testing environment, our rate table is designed to provide 360-degree continuous freedom in roll, pitch, and yaw axes. This extensive range of motion is essential to mimic the diverse flight patterns and maneuvers the UAV might undertake.

5.2 Positional Accuracy

A high positional accuracy of ± 0.1 degrees is targeted to ensure precision in the feedback system, allowing for accurate representations of flight dynamics during testing.

5.3 Angular Rates

To simulate the rapid maneuvers of high-speed target drones, we have established the following targets for angular rates:

- Roll Rate: 1800 deg/sec
- Pitch Rate: 1200 deg/sec
- Yaw Rate: 600 deg/sec

5.4 Load Capacity

The rate table will support a maximum load of 200 grams, allocated mainly for housing the MCU responsible for flight control.

5.5 Testbed Dimensions

To incorporate a Raspberry Pi for flight control effectively, we have set the maximum dimensions of the testbed to be 120x120mm. This size ensures a compact yet versatile platform to facilitate various testing configurations.

5.6 Justification of Specifications

The specified targets have been determined based on the flight dynamics of a kamikaze or other high-speed target drones. This approach ensures that our rate table can effectively mimic the rapid and diverse movements these drones are capable of. Moreover, considering the inclusion of a Raspberry Pi as the MCU for flight control, the load and testbed size have been optimized to accommodate this system, ensuring a reliable and efficient testing environment.

Chapter 6

Hardware Procurement Based on Target Specifications

In line with our predetermined target specifications, we undertook the task of procuring hardware that would not only meet but excel in satisfying the demands of our project. Below we detail the individual components and materials that were selected.

6.1 Gimbal BLDC Motors

We opted for high-performance gimbal BLDC outrunner motors, which emerged as an ideal choice for our project requirements given their exceptional adaptability and performance at low velocities. Here we detail the distinctive specifications and potential applications of the selected motors.

Gimbal motors are known for their incredibly smooth operations, marking them as an invaluable asset especially when precision and stability are required. These motors boast a high torque at low velocities, a feature that particularly benefits applications such as rate tables where maintaining a constant, slow speed is often vital. Their internal resistance, which is above 10Ω , and their ability to operate on currents up to 5A add to their efficiency and performance stability.

One of the notable advantages of using gimbal motors is their compatibility with any BLDC motor driver. Interestingly, they achieve comparable performance with both high and low-power BLDC motor drivers, a testament to their versatility and efficiency. This is mainly because high-performance drivers' current measurement circuits, optimized for high currents, don't offer any substantial benefit when utilized for gimbal motors, thus low-power drivers suffice. This attribute stood as a motivating factor in the de-

velopment of the SimpleFOCShield, allowing for a budget-friendly yet high-efficiency solution.

The array of applications where gimbal motors can be seamlessly integrated is expansive, encompassing realms from high-quality replacements for stepper or DC servo motors to smooth camera gimbals and various robotics applications. Their precision control and dynamic attributes even find utility in academic realms, serving as an impeccable tool in student experiments like ball and plate demonstrations, inverted pendulums, balancing robots, and similar setups requiring a high degree of control and dynamics.

In conclusion, the chosen gimbal BLDC motors not only cater to our immediate project requirements but also open avenues for versatile applications, promising smooth operations and high torque at low speeds.

Roll and Pitch Motors (Flycat 2805 140kv)

Specifications:

- Model: Flycat 2805 140kv
- Color: Black/Silver
- Dimensions: 34.5 x 14 mm
- Shaft hole diameter: 5.4 mm
- Weight: 41 ± 0.5 g
- Cable length: 9.5 cm

Description: This motor is chosen for its servo style connector that facilitates easy connections with gimbal controllers. It has a plug-and-play system with flexible cables for efficient balancing. The 2805 140KV Gimbal Brushless Motor is designed for a high power-to-weight ratio and is ideal for supporting GoPro class cameras weighing between 100 and 300g. Its lean profile allows for easy integration into setups, providing slop-free precision mounting through preloaded bearings.



Figure 6.1: Roll and Pitch Motors - Flycat 2805 140kv

Yaw Motor (iPower GM3506)

Specifications:

- Model: iPower GM3506
- Motor outer diameter: 40 ± 0.05 mm
- Motor height: 17.8 ± 0.2 mm (including encoder housing)
- Hollow shaft diameter: $12 - 0.008/-0.012$ mm (outer), $8.6 +0.05/0$ mm (inner)
- Wire length: 610 ± 3 mm
- Weight: 64 ± 0.2 g
- No-load current: 0.17 ± 0.05 A
- Working temperature range: -20 to 60°C

Description: The GM3506 by iPower is a robust brushless gimbal motor suitable for SLR and similar weight cameras, offering an impressive torque of 1.5KG/cm. Designed for substantial multi-rotor platforms aiming to lift SLR-sized gear, this motor ensures camera stability using brushless direct drive motors, providing a similar function to gimbals based on hobby servos.

6.2 Other Procured Hardware

In this section, we enumerate the various components procured to meet the demands of our project. Each item plays a crucial role in ensuring the successful realization of our UAV project. Below, we list these items along with brief descriptions:



Figure 6.2: Yaw Motor - iPower GM3506

- **IMU MPU 6050** - This unit is vital for obtaining the necessary inertial measurements to facilitate stable and controlled UAV flight. Detailed information on this component will be covered in the upcoming sections.
- **AS5600 Magnetic Position Sensor** - Employed for precise detection of the magnetic field, aiding in accurate positional awareness for the UAV. Its specifications and functionalities will be explored in detail in the subsequent sections.
- **Slip Rings** - These components facilitate the transmission of power and electrical signals from a stationary to a rotating structure, an essential feature in our rate table design. More details will follow in the later sections.
- **Ball Bearing** - These are employed to reduce rotational friction and to support radial and axial loads, playing a crucial role in ensuring the smooth operation of the Rate Table Joints



Figure 6.3: Other Included Hardware

6.2.1 Motor Drivers

Detailed specifications and features of the motor drivers used in the project are described in this section. These drivers are the brain and backbone of our rate table. These drivers have a node MCU ESP32 which acts as a Motor Controller. The Motor Controller reads the motor position from AS5600 Position Sensor and execute FOC code and based on that generate 3-phase PWM signals, which are then amplified via the Driver Chips. Current Sensors are also deployed in these drivers which measure the current from the motor which is required in our FOC algorithm.

Motor Driver for Roll and Pitch Motor

The MKS DUAL FOC Controller is a budget-friendly dual FOC drive control board designed with the ESP32 main control chip and based on the Apache 2.0 open-source protocol. The main specifications and features are as follows:

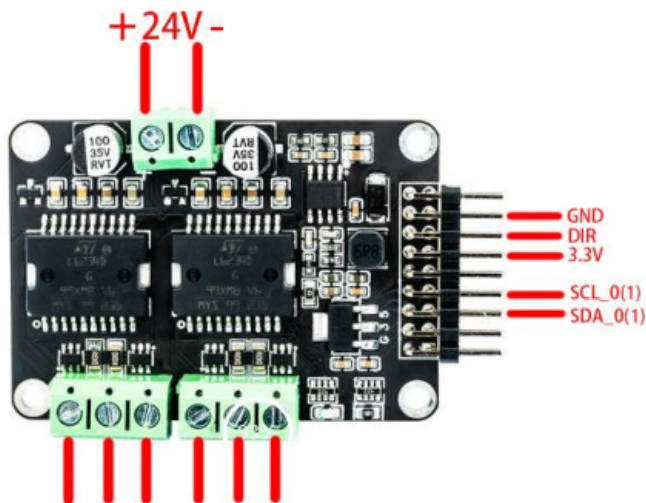


Figure 6.4: Motor Driver for Roll and Pitch Motor

- **Power:** 120 W per channel (dual: 240 W) with a supporting voltage range of 12 V-24 V.
- **Motor Compatibility:** Primarily designed for gimbal motors with a phase resistance greater than $10\ \Omega$.

- **Encoder Communication Methods:** Supports IIC, analog, ABI, and PWM methods.
- **External Control Methods:** Can be controlled via serial port or WIFI.
- **Maximum Motors Supported:** Can drive two motors simultaneously.

Motor Driver for Yaw Motor

This driver board supports both open and closed-loop control of FOC position, speed, and torque for most gimbal motors. Below are the details regarding its specifications and features:

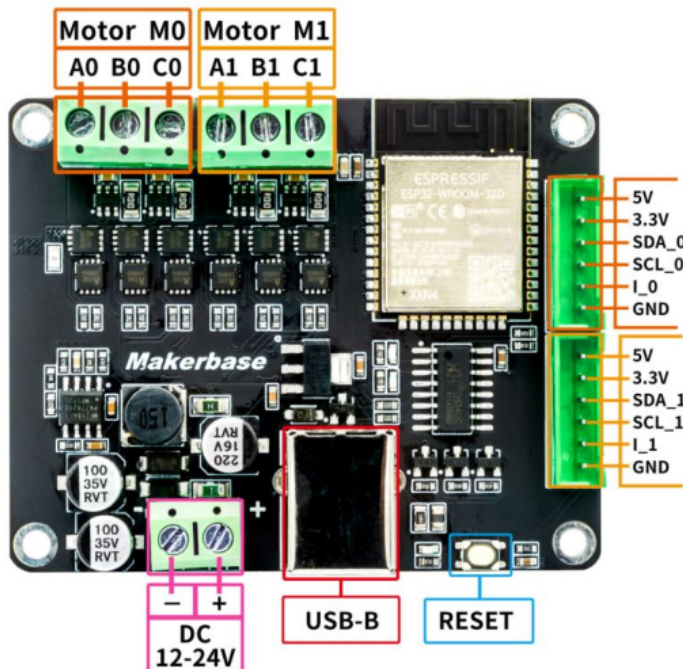


Figure 6.5: Motor Driver for Yaw Motor

- **Functionality:** Can potentially be expanded to support some aircraft model motors in the future.
- **Encoder Support:** Compatible with common IIC, ABI, PWM, HALL, and SPI formats.
- **Drive Circuit:** Includes two three-phase half-bridge drivers, each connected to the 3-way PWM control of ESP32.

- **Regulator Circuit:** Comprises of a DC-DC power supply IC and LDO, stabilizing the bus voltage to 5 V and 3.3 V respectively.
- **Interface:** Allows access to the remaining ports of the ESP32 development board for various functionalities, including power and encoder ports.
- **Dimensions:** 54.6 mm × 68.3 mm.
- **Voltage Range:** Operates within a voltage range of 12 V-24 V.
- **Current Handling:** Can handle a peak current of 12 A, with a single channel maximum of 6 A under optimal heat dissipation conditions.
- **Master Chip:** Built with the ESP32 WROOM 32D chip.
- **Current Sense Resistor:** Fitted with a 10 mR resistor, which can be replaced with a 1 mR to support specific aircraft model motors.

Each section provides a detailed insight into the technical specifications and functionalities, showcasing their crucial roles in the project's success.

6.3 3D Printing of Frames

The project also called for custom frames, which were created through a detailed process of 3D printing. This involved designing the frames using SolidWorks software, selecting the appropriate material for printing, and finally, bringing the design to life through the 3D printing process. The 3D printing not only allowed for a high degree of customization but also ensured that the frames were tailor-made to house all the procured hardware seamlessly, thus facilitating an efficient assembly process.

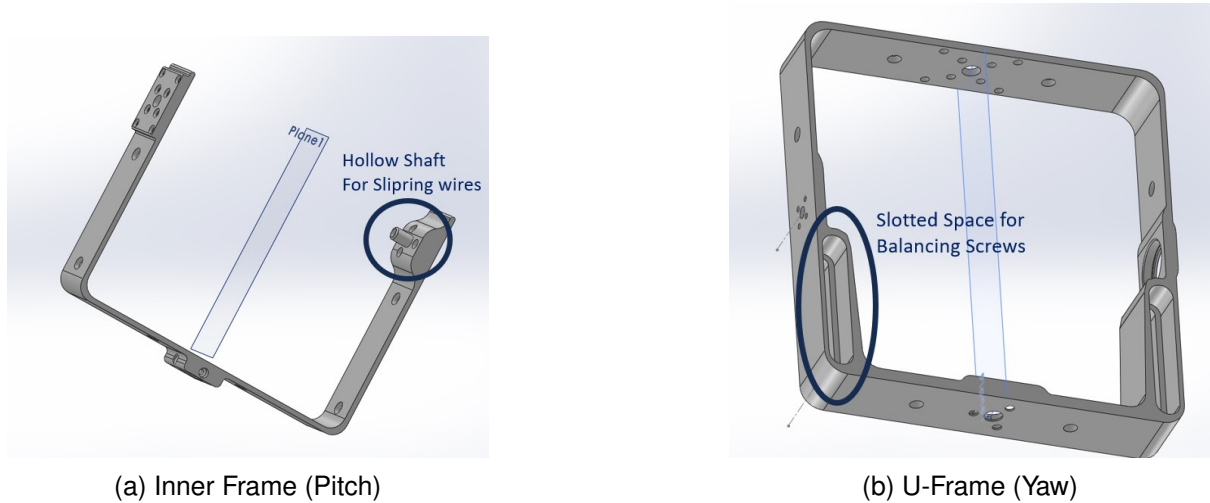


Figure 6.6: Components of the 3D Printed Frames

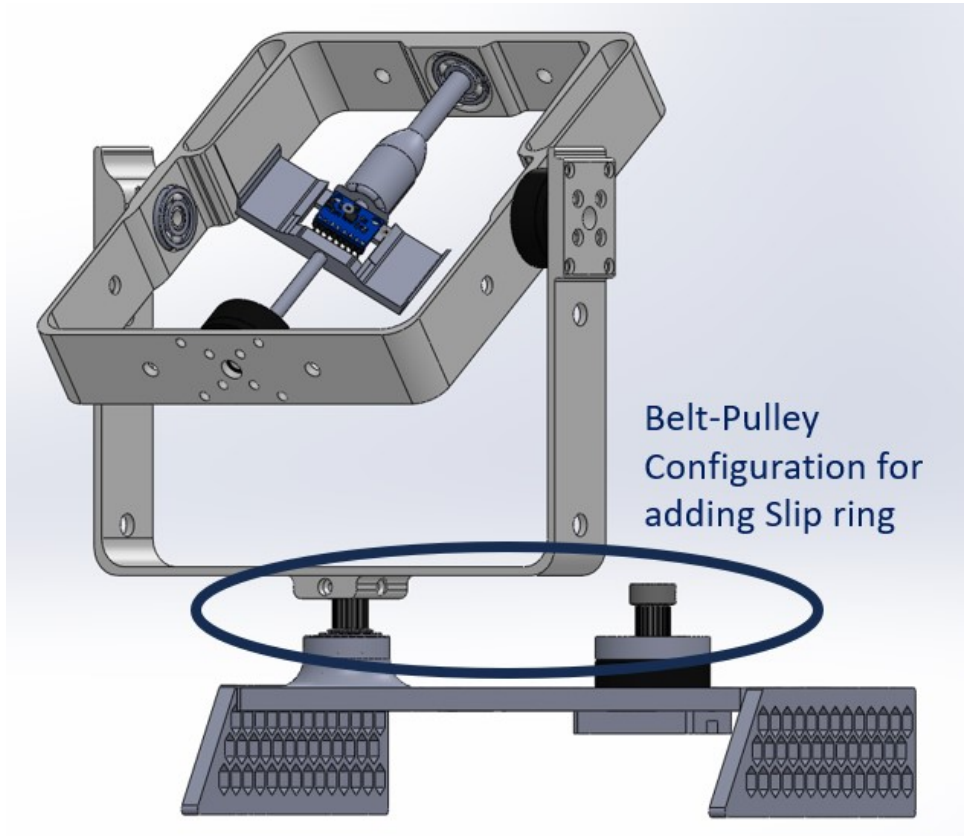


Figure 6.7: Final Assembly

Chapter 7

Implementation of Field-Oriented Control (FOC)

7.1 Closed-Loop Position Control

In this section, we focus on the core structure of the closed-loop position control mechanism, comprising three primary loops: the torque loop, the velocity loop, and the position loop. These loops intricately work together to facilitate a harmonious operation of the Field Oriented Control (FOC).

7.1.1 Torque Loop

The torque loop forms the foundational control level, directly influencing the motor's torque through varying control modes: voltage control mode, DC current mode, and FOC current mode. The more advanced the control mode is, the more exact torque control it offers, albeit requiring more potent microcontrollers and current sensing abilities.

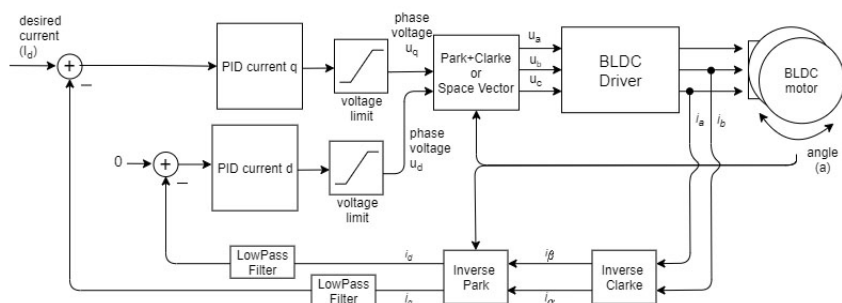


Figure 7.1: Torque Loop

7.1.2 Velocity Loop

Following the torque loop is the velocity loop, establishing control over the motor speed. It incorporates a PID velocity controller, effectively managing the torque targets to maintain user-set target velocity. Depending on the setup, it sets torque commands through voltage (U_q) or target currents (i_q).

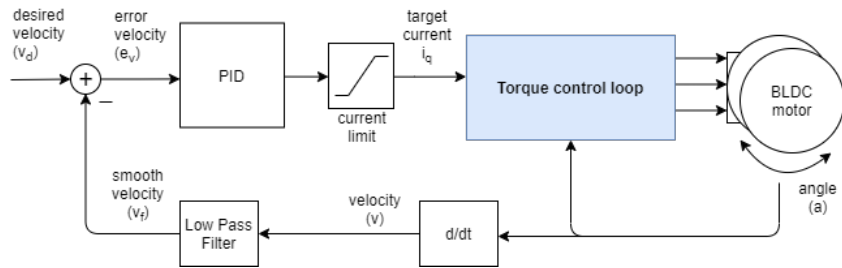


Figure 7.2: Velocity Loop

7.1.3 Position Loop

Finally, the position loop encapsulates the velocity loop, further narrowing down control to achieve precise rotor positioning. It introduces an additional control loop to the velocity loop, determining the necessary velocity and torque targets to reach and sustain the desired angular position as dictated by the user.

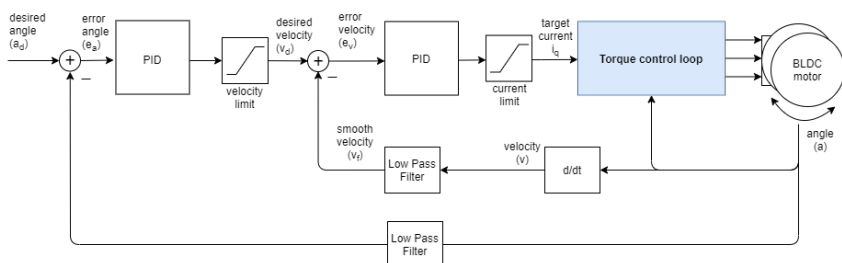


Figure 7.3: Position Loop

7.2 Motor Tuning

Motor tuning was carried out in a phased manner involving both open and closed-loop controls to optimize the motor's performance. This phased approach ensures the systematic progression through different tuning stages, each of which is explained below:

7.2.1 Open Loop Voltage Control

In this initial phase, the ideal voltage for each motor was determined to establish the foundation for subsequent tuning stages. This step is critical in setting up a stable and functional control system for the motors.

7.2.2 Open Loop Velocity Control

At this juncture, the velocity limits were verified to ensure the motor operates within safe and efficient boundaries. Understanding these limits is essential to maintaining the longevity and performance of the motor system.

7.2.3 Open Loop Position Control

Here, positional movements were scrutinized using the AS5600 sensor integrated at the back of each motor. This step verifies the accuracy and reliability of the positional feedback received from the sensors, establishing a ground truth for closed-loop control processes that follow.

7.2.4 Sensor Integration

Integration of the AS5600 sensor plays a pivotal role in fine-tuning the control loops. This process ensured the feedback systems are in place and functioning correctly before moving on to closed-loop controls.

7.2.5 Closed Loop Controls

The final stages of tuning involved closed-loop controls, assessed both with and without load, to fine-tune the motor performance under realistic operational conditions.

Closed Loop Velocity Control (no load)

In this step, the limits of the PID values of the velocity loop for each motor were determined under no load conditions, setting a baseline for loaded tests.

Closed Loop Position Control (no load)

Here, the PID values for the position loop of each motor were scrutinized, determining the optimum parameters for stable and efficient control in no load conditions.

Closed Loop Velocity Control (with load)

During this phase, ideal PID values were established through trial and error in the final assembly. The 'P' value was adjusted to facilitate motor movement at 70-75% of the target velocity, while the 'I' value covered the remaining 25-30%. It was observed that the 'D' value was not essential in this setup.

Closed Loop Position Control (with load)

In the final stage, acceleration limits were instituted, and the motors were calibrated to attain a target position of 1 rad in the minimum possible time, while maintaining stability and minimal overshoot. This fine-tuning ensures optimal performance in real-world operating conditions.

7.3 Final PID Values

In this section, we will present the finalized PID values derived from the meticulous motor tuning process, serving as the cornerstone for achieving the desired motor performance.

7.3.1 Roll Motor

- Velocity Loop:
 - P: 0.1
 - I: 3
- Angle Loop:
 - P: 5
- Low Pass Filter (LPF) Time Constant (Tf): 0.01
- Voltage Limit: 5 V

- Velocity Limit: 20 rad/s

7.3.2 Pitch Motor

- Velocity Loop:
 - P: 1
 - I: 3
- Angle Loop:
 - P: 5
- Low Pass Filter (LPF) Time Constant (Tf): 0.01
- Voltage Limit: 5 V
- Velocity Limit: 15 rad/s

7.3.3 Yaw Motor

- Velocity Loop:
 - P: 0.5
 - I: 2
- Angle Loop:
 - P: 5
- Low Pass Filter (LPF) Time Constant (Tf): 0.01
- Voltage Limit: 3 V
- Velocity Limit: 10 rad/s

7.4 Motor Tuning Results

To provide a comprehensive view of the motor tuning results, below are the step response for 1 rad position for yaw motor with and without load.

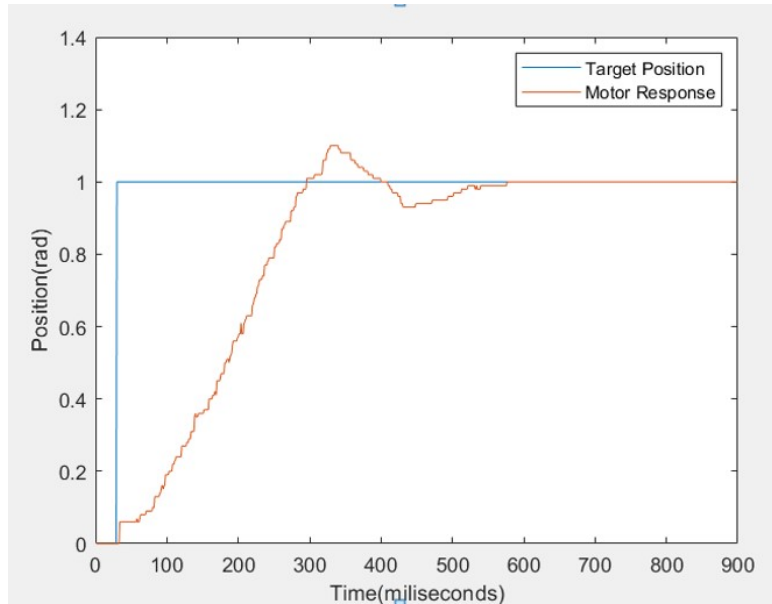


Figure 7.4: Yaw Motor (No Load)

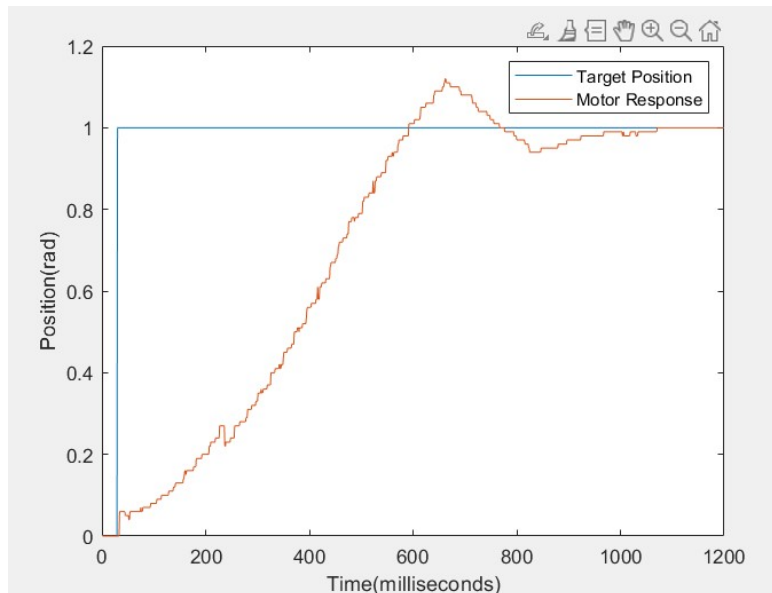


Figure 7.5: Yaw Motor (With Load via Belt-Pulley Configuration)

7.4.1 Discussion

The motor tuning process revealed a significant overshoot during the 'with load' tests. This overshoot is largely attributable to the belt-pulley configuration utilized in our setup, which inherently is not designed to accommodate high accelerations, especially in the context of simulating the yaw motor.

While this configuration serves well in imitating the yaw motor's behavior, it introduces certain limitations when subjected to high accelerations, thereby causing over-

shoots. It is important to note that despite these overshoots, the system maintains a satisfactory level of performance, meeting the requisite operational benchmarks set for the yaw motor.

FOC Code

This is the code deployed in Motor Controller 1 which is controlling Pitch and Roll Motors

Including the Library

```
1 #include <SimpleFOC.h>
```

This line includes the SimpleFOC library which contains the classes and functions necessary for setting up and controlling your BLDC motors.

Setting Up Sensors, Drivers, and Motors

```
1 InlineCurrentSense current_sense = InlineCurrentSense(0.01, 20, 39, _NC, 36);
2 InlineCurrentSense current_sense1 = InlineCurrentSense(0.01, 20, 35, _NC, 34);
```

In this part of the code, two objects of the ‘InlineCurrentSense’ class are created to handle the current sensing for each motor. The parameters provided to the constructors are used to configure the current sensing setup.

Magnetic Sensors and I2C Configuration

```
1 MagneticSensorI2C sensor = MagneticSensorI2C(AS5600_I2C);
2 MagneticSensorI2C sensor1 = MagneticSensorI2C(AS5600_I2C);
3 TwoWire I2Cone = TwoWire(0);
4 TwoWire I2Ctwo = TwoWire(1);
```

In this section, magnetic sensors and I2C communication lines are set up for each motor. The ‘AS5600’ sensors use I2C for communication, and two separate ‘TwoWire’ objects are initiated to facilitate this communication.

Motor Parameters and Driver Initialization

Here you will detail the initial setup of the motors and drivers by initializing the ‘BLDC-Motor’ and ‘BLDCDriver3PWM’ objects with appropriate parameters and linking them together.

```

1 //Command settings
2 float target_velocity = 0;
3 float target_velocity1 = 0;
4
5 Commander command = Commander(Serial);
6 void doTarget(char* cmd) { command.scalar(&target_velocity, cmd); }
7 void doTarget1(char* cmd) { command.scalar(&target_velocity1, cmd); }
```

In this subsection, the target velocities for both the pitch and roll motors are initialized to zero. The ‘Commander’ object is also initialized with the Serial object for communication. Two functions, ‘doTarget’ and ‘doTarget1’, are defined to modify the target velocities based on the commands received through the serial interface.

Setup Function

```

1 void setup() {
2     I2Cone.begin(19,18, 400000);
3     I2Ctwo.begin(23,5, 400000);
4     sensor.init(&I2Cone);
5     sensor1.init(&I2Ctwo);
6
7     // linking and initializing other setups such as sensor linking,
8     // driver initialization, FOC modulation setup, and PID setups.
9
10    motor.linkSensor(&sensor);
11    motor1.linkSensor(&sensor1);
12
13    // Voltage settings, motor linking, modulation and control type setup
14    driver.voltage_power_supply = 12;
15    driver.init();
16    current_sense.linkDriver(&driver);
17    driver1.voltage_power_supply = 12;
18    driver1.init();
19    current_sense1.linkDriver(&driver1);
20    motor.linkDriver(&driver);
21    motor1.linkDriver(&driver1);
22    motor.foc_modulation = FOCModulationType::SpaceVectorPWM;
23    motor1.foc_modulation = FOCModulationType::SpaceVectorPWM;
24    motor.controller = MotionControlType::angle;
25    motor1.controller = MotionControlType::angle;
26
```

RESTRICTED

```
27 // PID setups
28 motor.PID_velocity.P = 1;
29 motor1.PID_velocity.P = 0.5;
30 motor.PID_velocity.I = 3;
31 motor1.PID_velocity.I = 3;
32 motor.P_angle.P = 5;
33 motor1.P_angle.P = 5;
34 motor.voltage_limit = 5;
35 motor1.voltage_limit = 5;
36 motor.current_limit = 1;
37 motor1.current_limit = 0.5;
38 motor.voltage_sensor_align = 3;
39 motor1.voltage_sensor_align = 3;
40
41 motor.sensor_offset= -0.66;
42 motor1.sensor_offset= 2.54;
43
44 //Speed low-pass filter time constant
45 motor.LPF_velocity.Tf = 0.01;
46 motor1.LPF_velocity.Tf = 0.01;
47
48 //Set a maximum speed limit
49 motor.velocity_limit = 15;
50 motor1.velocity_limit = 20;
51
52 motor.motion_downsample = 5;
53 motor1.motion_downsample = 5;
54
55 Serial.begin(115200);
56 motor.useMonitoring(Serial);
57 motor1.useMonitoring(Serial);
58
59 motor.init();
60 motor1.init();
61
62 current_sense.init();
63 current_sense1.init();
64
65 motor.linkCurrentSense(&current_sense);
66 motor1.linkCurrentSense(&current_sense1);
67 //Initialize FOC
68 motor.initFOC(0.72404, Direction::CW);
69
70 motor1.initFOC(2.60, Direction::CW);
71
72 command.add('P', doTarget, "target velocity");
73 command.add('R', doTarget1, "target velocity");
74
75 Serial.println(F("Motor ready."));
76 Serial.println(F("Set the target velocity using serial terminal:"));
77 }
```

In this subsection, the ‘setup’ function is detailed. The function begins with the initialization of two I2C communication lines with specified pin numbers and frequency. Following this, sensors and motors are initialized and linked appropriately, and various motor parameters including voltage settings and control types are configured. PID control settings for velocity and angle control are also set up within this function.

Loop Function

```
1 void loop() {  
2     Serial.print("P");  
3     Serial.print(sensor.getAngle()+0.66);  
4     Serial.print(",");  
5     Serial.print("R");  
6     Serial.print(sensor1.getAngle()-2.54);  
7     Serial.println();  
8     motor.loopFOC();  
9     motor1.loopFOC();  
10  
11    motor.move(target_velocity);  
12    motor1.move(target_velocity1);  
13  
14    command.run();  
15 }
```

In this section, the ‘loop’ function is outlined, which is executed indefinitely in a loop. Inside this function, the angles of both sensors are printed to the serial monitor with necessary adjustments. The FOC loop is executed for both motors using their respective ‘loopFOC’ methods, and the ‘move’ method is called on both motors with their respective target velocities. Finally, any pending serial commands are executed with the ‘run’ method of the ‘Commander’ object. [17]

Chapter 8

Preparing for HILS

Hardware-in-the-Loop Simulation (HILS) is a technique used in the development and testing of complex real-time embedded systems. In this chapter, we will detail the steps involved in setting up a HILS environment with a focus on the integration of an IMU MPU-6050 sensor on a rate table testbed.

8.1 IMU MPU-6050 Setup on Testbed

The first step in preparing for HILS is placing the IMU MPU-6050 sensor on the testbed of the rate table. The MPU-6050 is a sensitive device that can detect changes in pitch, roll, and yaw angles.

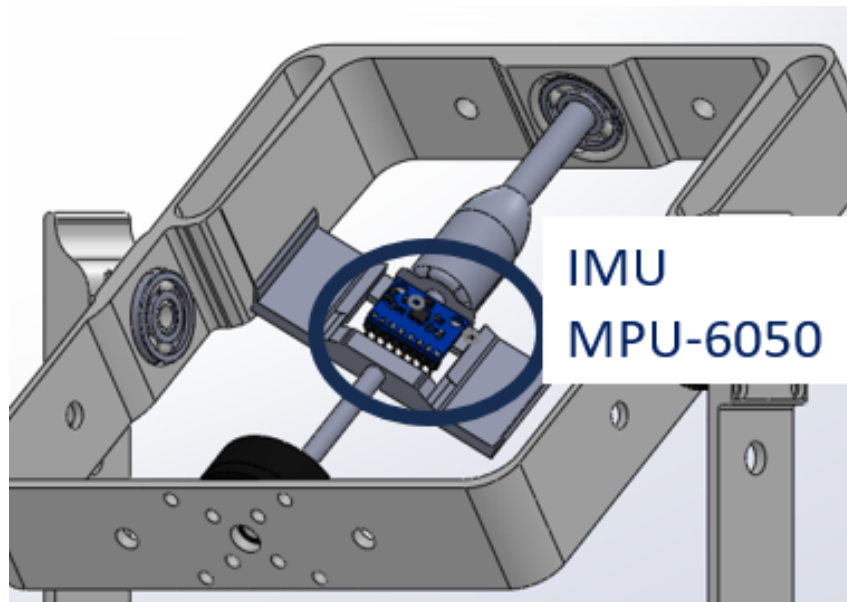


Figure 8.1: Location of the IMU MPU-6050 on the testbed

Refer to Figure 8.1 for the detailed setup. Once placed appropriately on the testbed,

it should be calibrated to ensure accurate readings.

8.2 Accessing IMU Values Via WiFi

After the IMU is set up, it is necessary to configure it to transmit the data via WiFi. This configuration allows the IMU values to be accessed remotely through a UDP signal. Detailed steps on setting up the WiFi and UDP configuration will be covered in subsequent sections.

8.3 Hardware in Loop Simulation Block Diagram

Understanding the HILS block diagram is crucial for setting up a successful simulation environment. The diagram illustrates the complete flow of data and control signals in the simulation loop, helping to pinpoint areas where potential issues might arise during the testing phase.

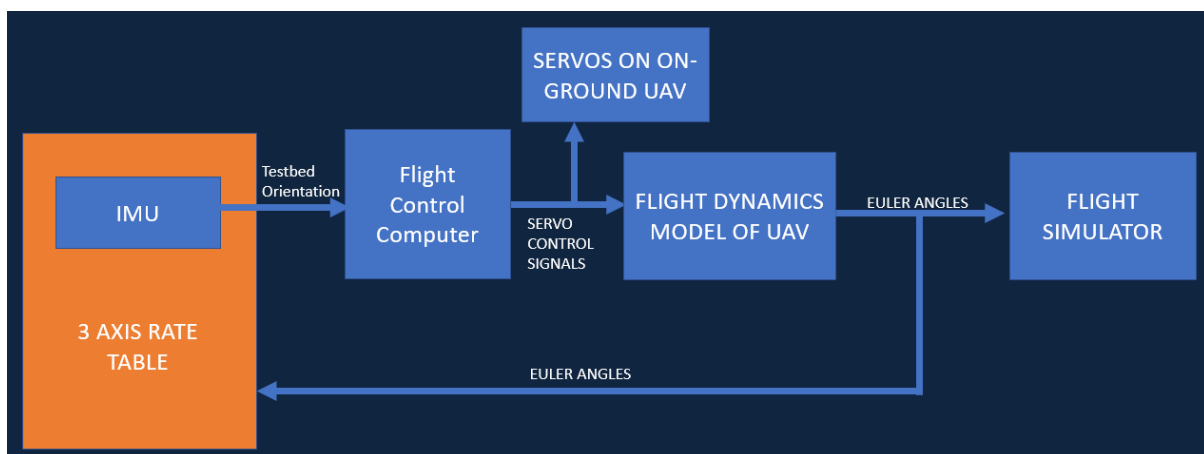


Figure 8.2: Hardware in Loop Simulation Block Diagram

Refer to Figure 8.2 to understand the intricate details of a HILS setup.

Chapter 9

Final Results

In the culmination of our project, we successfully achieved a functioning hardware setup. The meticulously crafted testbed demonstrated the ability to roll, pitch, and yaw, both individually and synchronously, thus embodying the intricate maneuvers possible in a flight scenario.

A pivotal aspect of our success was the seamless integration with Flight Gear. This integration facilitated an almost mirrored reflection of the simulation, enhancing the realism and fluidity of the aircraft's movement as displayed in Flight Gear.

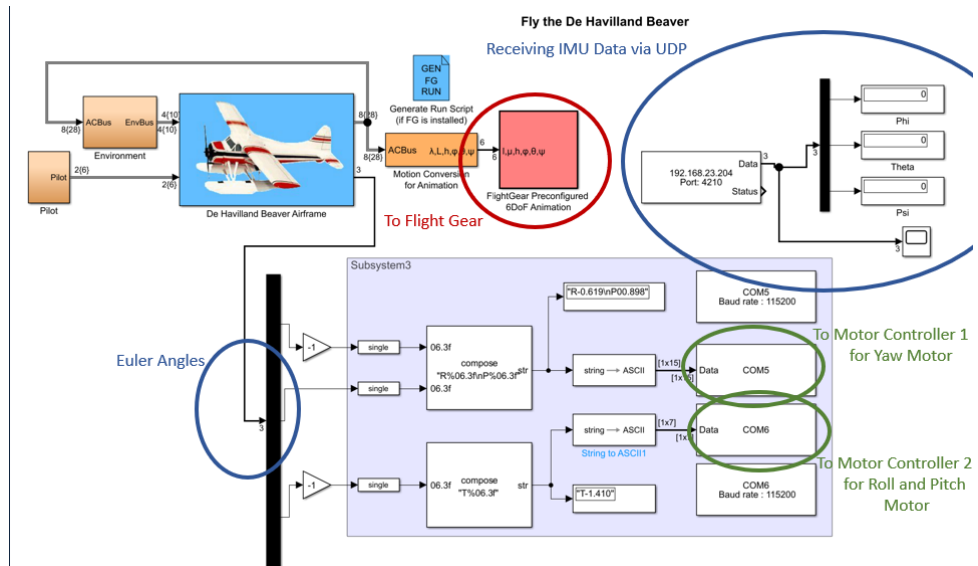


Figure 9.1: Integration of Rate Table (Hardware) with Flight Gear

This congruent setup, synthesizing the physical actions of the hardware with the virtual representation in Flight Gear, symbolizes a significant milestone in our project, offering a tangible and dynamic representation of our theoretical work over the project's duration.

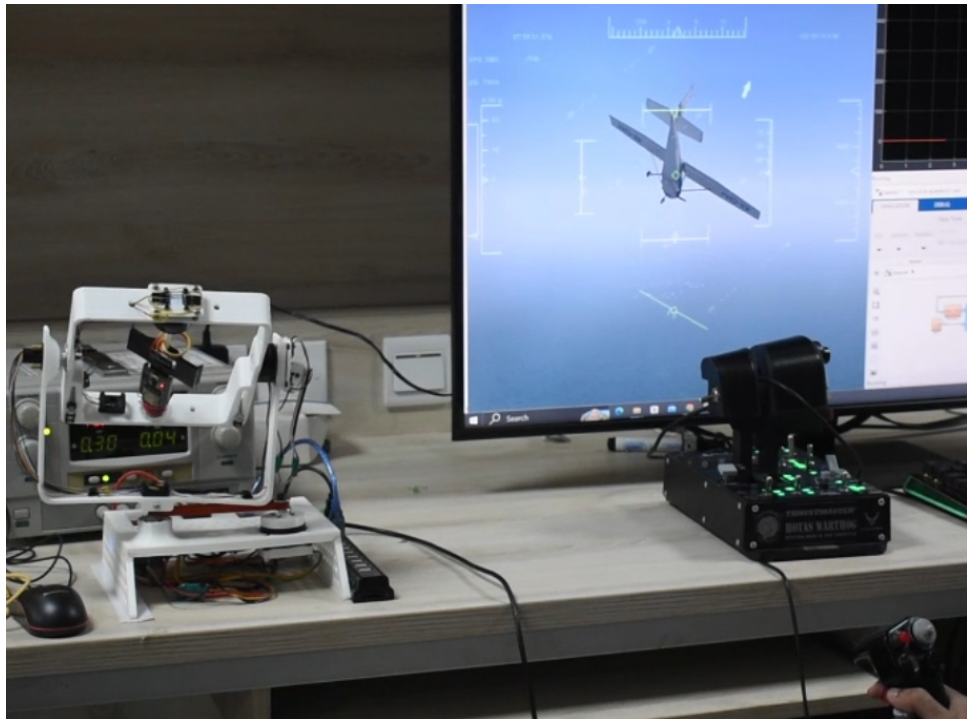


Figure 9.2: Rate Table Demonstration

Figure 9.2 vividly illustrates the integration achieved, showcasing the harmony between the hardware and Flight Gear. The meticulous synchronization of the Rate Table's physical movements with the software simulation offers viewers a vivid and immersive experience, serving as a testament to the project's success and the potent potential for further explorations and advancements in this domain.

In retrospect, the journey from conceptualization to realization has been both challenging and rewarding. Every milestone achieved, and every hurdle overcome has led to this moment of fruition, where the physical intertwines with the virtual, crafting a symphony of synchronized movements, opening avenues for explorations in flight simulations that are closer to reality than ever before.

Chapter 10

Future Recommendations

As we forge ahead, envisaging the next phases of this project, we find it incumbent upon ourselves to delineate potential pathways and opportunities for further enhancement and development. Here, we outline several pivotal areas where future endeavors can concentrate, to elevate the project to new heights:

10.1 Design Adaptations for Heavier Payloads

Future iterations of the project should focus on design adaptations necessary to facilitate heavier payloads, potentially up to 5kg. This encompasses reinforcing the structure to withstand increased weight while maintaining the dynamism and functionality integral to the operation of the simulator.

10.2 Lab Equipment for Testing and Validation

Investing in dedicated lab equipment for meticulous testing and validation of various components including FCC, FDM, and sensors is essential. This would pave the way for more precise and accurate simulations, fostering a more reliable and trustworthy system.

10.3 Division of Project into Mechanical and Control Design

To streamline the workflow and foster specialization, the project can be bifurcated into two primary realms: Mechanical and Control Design. This approach would encourage

a deeper focus and expertise in both segments, enhancing the overall output and efficiency.

10.4 Integration of Superior Sensors

The adoption of better sensors equipped with SPI interface or ABZ encoders can be a significant upgrade, offering finer control and feedback, thus enhancing the responsiveness and accuracy of the system.



Figure 10.1: Rotary ABZ Encoder

10.5 Utilization of Motors with More Poles

Engaging motors with a higher number of poles can potentially facilitate smoother and more nuanced control over movements, paving the way for a more fluid and realistic simulation experience.



Figure 10.2: GM-8112 Gimbal Motor with 42 Poles

10.6 Odrive Motor Controllers

Integrating Odrive motor controllers can be a substantial uplift, offering more sophisticated control and anticogging features with a STM32 powerful core, hence improving the finesse and precision in motor control.

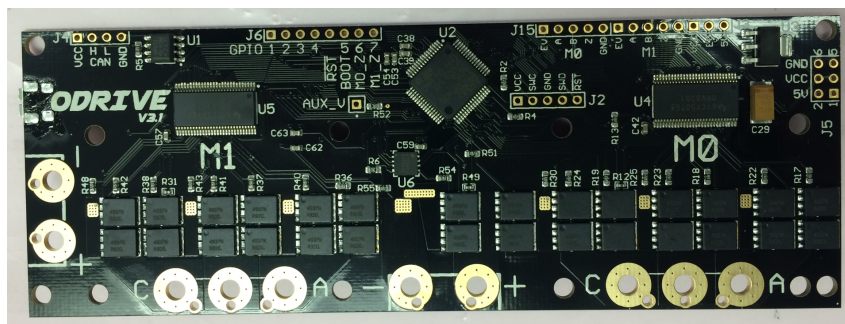


Figure 10.3: Odrive Motor Controller

10.7 Incorporation of Industrial Slip Rings/Ball Bearings

To foster a seamless connection and integration of various equipment on the testbed, incorporating industrial-grade slip rings and ball bearings with increased channel capacity is essential. This would ensure a more robust and reliable connection, enhancing the overall stability and performance of the system, and providing adequate wires

to the testbed for connecting and testing payloads.

10.8 Integration of High Precision IMU

The implementation of a high-precision IMU (Inertial Measurement Unit) would bolster the simulator's performance by providing more accurate and responsive feedback on the system's dynamics, thus allowing for a more realistic and immersive simulation experience.

In conclusion, the path ahead is replete with opportunities for growth and refinement. By focusing on these crucial areas of development, future teams can build upon the solid foundation laid, steering the proof of concept product to a final product.

Chapter 11

Conclusion

In this paper, we embarked on a deep exploration of the construction and utility of 3-axis rotary tables, a vital asset in the sectors of aerospace and defense. The in-depth analysis carried encompassed a gamut of components and functionalities ranging from the meticulous configuration of Euler angles to the pioneering realm of Field Oriented Control (FOC). A substantial segment of the discourse delved into the advanced sensor technologies such as MEMS-based IMUs and magnetic encoders, illuminating their cardinal role in enhancing the precision and accuracy of the rotary tables.

In concurrence with the global strides in computational technologies, the discussion underscored the incorporation of cutting-edge technological advancements, highlighting their instrumental role in elevating the performance metrics of sensors and subsystems in testing environments. Through the meticulous design and optimization processes outlined in preceding chapters, we have illustrated the roadmap to forging a rotary table capable of real-time testing and validation in controlled environments, fostering notable advancements in hardware-in-loop simulations and facilitating interfaces with contemporary technologies like Inertial Navigation Systems (INS) and Attitude Heading Reference Systems (AHRS).

In the context of Pakistan's accelerating development in autonomous airborne platforms, the pertinence of this project resonates profoundly. As civil and military sectors, represented by firms like GIDS, DESTO, POF, and PAC, steer towards an autonomous future, the demands for efficient and cost-effective testbeds for HILS have surged. The inception of a homegrown testbed, delineated in this project, stands as a beacon of promise, heralding a future where versatility meets cost-efficiency, potentially saving millions while offering adaptability to various requirements.

RESTRICTED

In synthesis, this project not only elucidates a pathway to a sophisticated and versatile 3-axis rotary table but also anchors itself firmly in the national narrative, answering a pressing call for innovation in the burgeoning aerospace and defense sectors in Pakistan. Thus, we forward a venture steeped in potential, beckoning a future of indigenous technological advancement, one grounded in precision, efficiency, and national self-reliance.

Bibliography

- [1] ETS Solutions Asia Pacific. Tmc rate tables.
- [2] Phillip Denne. Motion platforms or motion seats. *Published September, 2004.*
- [3] Wei Dong, Zhijiang Du, Yongqiang Xiao, and Xiaoguang Chen. Development of a parallel kinematic motion simulator platform. *Mechatronics*, 23(1):154–161, 2013.
- [4] Hassen Nigatu, Yun Ho Choi, and Doik Kim. Analysis of parasitic motion with the constraint embedded jacobian for a 3-prs parallel manipulator. *Mechanism and Machine Theory*, 164:104409, 2021.
- [5] Xie Yue, M. Vilathgamuwa, K.J. Tseng, and N. Nagarajan. Modeling and robust adaptive control of a 3-axis motion simulator. In *Conference Record of the 2001 IEEE Industry Applications Conference. 36th IAS Annual Meeting (Cat. No.01CH37248)*, volume 1, pages 553–560 vol.1, 2001.
- [6] Tarun Agarwal. Different types of electric motors and their applications, Jul 2019.
- [7] Chang-liang Xia. *Permanent magnet brushless DC motor drives and controls*. John Wiley & Sons, 2012.
- [8] Freescale Semiconductors. Bldc motor control with hall sensor based on frdm-ke02z - nxp.
- [9] Meghana N Gujar and Pradeep Kumar. Comparative analysis of field oriented control of bldc motor using spwm and svpwm techniques. pages 924–929, 2017.
- [10] Eka Firmansyah, Fransisco Danang Wijaya, W. P. Rendy Aditya, and Ridwan Wicaksono. Six-step commutation with round robin state machine to alleviate

RESTRICTED

- error in hall-effect-sensor reading for bldc motor control. *2014 International Conference on Electrical Engineering and Computer Science (ICEECS)*, pages 251–253, 2014.
- [11] Kh.I. Saleh, M.A. Badr, and S.A. Wahsh. Perfect field oriented brushless dc motor. In *2001 Power Engineering Society Summer Meeting. Conference Proceedings (Cat. No.01CH37262)*, volume 3, pages 1433–1438 vol.3, 2001.
 - [12] Marek Lazor and Marek Štulrajter. Modified field oriented control for smooth torque operation of a bldc motor. In *2014 ELEKTRO*, pages 180–185, 2014.
 - [13] Debjyoti Chowdhury, Madhurima Chattopadhyay, and Priyanka Roy. Modelling and simulation of cost effective sensorless drive for brushless dc motor. *Procedia Technology*, 10:279–286, 2013.
 - [14] Shiyong Lee, Tom Lemley, and Gene Keohane. A comparison study of the commutation methods for the three-phase permanent magnet brushless dc motor. pages 49–55, 2009.
 - [15] Bo Li and Chen Wang. Comparative analysis on pmsm control system based on spwm and svpwm. In *2016 Chinese Control and Decision Conference (CCDC)*, pages 5071–5075, 2016.
 - [16] Deepak Mohanraj, Ranjeev Aruldavid, Rajesh Verma, K Sathyasekar, Abdulwasa Bakr Barnawi, Bharatiraja Chokkalingam, and Lucian Mihet-Popa. A review of bldc motor: State of art, advanced control techniques, and applications. *IEEE Access*, 2022.
 - [17] Antun Skuric, Hasan Sinan Bank, Richard Unger, Owen Williams, and David González-Reyes. Simplefoc: A field oriented control (foc) library for controlling brushless direct current (bldc) and stepper motors. *Journal of Open Source Software*, 7(74):4232, 2022.